NASA CR-935

DYNAMIC STABILITY OF SPACE VEHICLES

Volume I - Lateral Vibration Modes

By G. B. Paddock

Issued by Originator as Report No. GD/C DDF 65-001

Prepared under Contract No. NAS 8-11486 by
GENERAL DYNAMICS CORPORATION
San Diego, Calif.

for George C. Marshall Space Flight Center

NATIONAL AERONAUTICS AND SPACE ADMINISTRATION

For sale by the Clearinghouse for Federal Scientific and Technical Information
Springfield, Virginia 22151 – CFSTI price $3.00

FOREWORD

This report is one of a series in the field of structural dynamics prepared under contract NAS 8-11486. The series of reports is intended to illustrate methods used to determine parameters required for the design and analysis of flight control systems of space vehicles. Below is a complete list of the reports of the series.

Volume I	Lateral Vibration Modes
Volume II	Determination of Longitudinal Vibration Modes
Volume III	Torsional Vibration Modes
Volume IV	Full Scale Testing for Flight Control Parameters
Volume V	Impedence Testing for Flight Control Parameters
Volume VI	Full Scale Dynamic Testing for Mode Determination
Volume VII	The Dynamics of Liquids in Fixed and Moving Containers
Volume VIII	Atmospheric Disturbances that Affect Flight Control Analysis
Volume IX	The Effect of Liftoff Dynamics on Launch Vehicle Stability and Control
Volume X	Exit Stability
Volume XI	Entry Disturbance and Control
Volume XII	Re-entry Vehicle Landing Ability and Control
Volume XIII	Aerodynamic Model Tests for Control Parameters Determination
Volume XIV	Testing for Booster Propellant Sloshing Parameters
Volume XV	Shell Dynamics with Special Applications to Control Problems

The work was conducted under the direction of Clyde D. Baker and George F. McDonough, Aero Astro Dynamics Laboratory, George C. Marshall Space Flight Center. The General Dynamics Convair Program was conducted under the direction of David R. Lukens.

TABLE OF CONTENTS

LIST OF ILLUSTRATIONS

LIST OF TABLES

NOMENCLATURE

A	cross sectional area
C	flexibility matrix
D	dynamic matrix
E	Young's modulus
F	Generalized forces - non zero generalized displacements
G	Shear modulus
f	function , e. g. f (x) or frequency
H	axial load
I	area moment of inertia
I_a	mass moment of inertia
I_T	total mass inertia about fixity point
i	coordinate index
j	coordinate index
K	stiffness matrix
k	element stiffness, spring rate
L	distance to center of gravity
l	beam length
M	mass matrix; external moment; total moment
M_T	total mass
m	element mass, incremental moment
n	mode index
P	external lateral force; total lateral force
p	incremental lateral force
Q	generalized force

q	normal mode coordinate
R	incremental load, total load transform matrix
r	deflection shape trial index
S	static moment about fixity point
T	relative displacement /absolute displacement transform matrix
t	time
U	deflection amplitude
V	shear
w_o	displacement of fixity point upon release
x	displacement along neutral axis
Y	rigid body lateral displacement
y	displacement normal to neutral axis
$\bar{y}$	relative displacement
z	displacement in general case
α	modal bending slope
β	total modal slope
γ	modal shear slope
Δ	connecting element deformation - mode synthesis
ζ	generalized displacements - zero generalized forces
η	modal weighting factor - mode synthesis
Θ	rigid body rotation
θ	rotary displacement
λ	eigenvalue
μ	mass per unit length
υ_o	rotation of fixity point upon release
ξ	damping factor
ρ	generalized displacement
Φ	matrix of mode shapes
φ	modal displacements
ψ	eigenvector
ω	natural circular frequency

a, $\bar{a}$, b, $\bar{b}$, c, $\bar{c}$, d, $\bar{d}$, e, g, w^2, v^2, W are mathematical expressions defined in the text.

$(\dot{})$	a dot over a symbol indicates first time derivative
$(\ddot{})$	two dots over a symbol indicates second time derivative
$[\ ]$	square matrix
$[\ ]$	diagonal matrix
$\{\ \}$	column matrix

1/INTRODUCTION

This monograph discusses the lateral model development and modal calculations for the cylindrical space vehicle system and also systems employing clustered tanks. Relative importance of physical characteristics will be discussed as well as methods used by the industry for the solution of modal parameters. Primary attention is focused on parameters important in control and stability analyses for which the system frequency of interest is generally below twenty cycles per second and quite often below ten cycles per second. Application for loads analysis follows the same principals outlined herein but may require more detailed representation in areas where loads or deflections can be critical. The models described will be concerned with gross vehicle lateral motions and will not include the shell radial deflection modes which can be significant for local effects analysis but generally do not contribute to gross vehicle control and stability. Related monographs describe torsional, longitudinal, and sloshing models. Stability and loads analytical methods using these models and modal parameters are also subjects of other monographs.

The general approach for dynamic solutions involving large systems is to develop a mathematical model describing the system's mass and structure, calculate its normal modes of vibration, and then, using normal mode theory, apply the external forces and couple in the control system to obtain total response. The dynamic analysis is then only as accurate as provided by the mathematical model representing the space vehicle system; therefore, development of these models is of major importance in dynamic analysis. Also, since these models are idealizations and approximations of the real system, the experience of an analyst in deciding which elements are dominant contributes greatly to the successful representation of the system.

Representation of the space vehicle system in the lateral direction is accomplished by a series of lumped masses connected by elastic beams. By successive refinements, such as branch beams to include multiple load paths, concentrated masses attached to the beam by translational and rotational springs, or other possible independent structures or components, the model can simulate all significant motions. The mathematical model and numerical techniques to obtain lateral normal modes for space vehicle systems comprised of tandem cylindrical structures have been extensively developed by aerospace industries.

The addition of peripheral tanks to a center core increases the complexity by three mechanisms: (1) the attachments between tanks require additional boundary conditions: (2) the attaching structure is generally complex, and (3) the peripheral tanks generally destroy axis-symmetry and results in multi-directional normal modes. The present techniques employed with these clustered boosters are essentially the same as those of the simple cylindrical structure; however, the complexity dictates use of more points to describe the system and the analysis can easily exceed computer storage capacity. This leads to a compromise between accuracy of results and efficiency and capability of present computer facilities.

2/STATE-OF-THE-ART

The original work in the study of the phenomenon of structural dynamic behavior was primarily restricted to simple spring-mass systems and severly limited in its coverage of continuous systems to uniform beams and plates. As structural complexity increased, consideration of practicality rendered these solutions unjustified. The analysis of larger systems required vast amounts of time and effort and, since all calculations were done by hand, numerical accuracy became a problem of major concern. The most practical solution to a structural dynamics problem generally turned out to be a healthy factor of safety applied to structural capacity.

With the advent of aircraft, a large safety factor could no longer provide the means of accomodating dynamic effects. The development of machine calculators enabled the analyst to develop more complex dynamic models and associated solution techniques to provide answers to the problems of stability and flutter in aircraft design. Still further refinement in modeling techniques has been permitted by the introduction of electronic computing systems. The capacity of these computing systems and rapid computation cycles has resulted in the development of more numerical techniques utilizing smaller iteration intervals with a resultant increases in solution accuracy.

Approximate methods for solving the equations resultant from model simulations have been developed; a summary (from Reference 1) in tabular form of the representative accuracy of some of these techniques is presented in Table 1.

To illustrate the ability of lumped parameter systems to represent continuous systems, consider a uniform simply supported beam. The exact expressions for the natural frequencies and their associated mode shapes are well known:

$$\omega^2 = \left(\frac{n\pi}{l}\right)^4 \frac{EI}{\mu}$$

$$\psi_n = \text{Sin}\,\frac{n\pi x}{l}$$

where n is mode number, l is the length of the beam, and μ is the mass per unit length. Assuming the following physical data:

l = 120 inches (3.05 meters)

$EI = 8 \times 10^9$ lb-in^2 (2.33×10^{13} gr cm^2)

μ = 400 lb/inch (7.14×10^4 gr/cm)

the resultant first three natural frequencies are:

$\omega_1^2 = 3626.5$; $\omega_1 = 60.22$; f = 9.58 cps

$\omega_2^2 = 58024.$; $\omega_2 = 240.88$; f = 38.34 cps

$\omega_3^2 = 293748.$; $\omega_3 = 541.98$; f = 86.26 cps

Table 1. Comparison of Accuracy of Various Methods of Approximate Solution

Method	Number of Masses	ω_1	% Error	ω_2	% Error
Rayleigh-Ritz 2-Polynomial	10	2.5372	2.38	12.9085	42.0
Rayleigh-Ritz 3-Polynomial	10	2.4894	0.45	9.9379	9.34
Modified Rayleigh-Ritz 2-Polynomial	10	2.4769	-0.05	9.4832	4.34
Collocation	11	2.4760	-0.09	8.9207	-1.85
2 Station Functions	11	2.4773	-0.04	9.0012	-0.96
Iterated Rayleigh-Ritz Polynomial (Galerkin)	10	2.4769	-0.05	9.4832	4.34
Holzer-Myklestad	10	2.4776	-0.02	9.1513	0.69
Direct Iteration	5	2.4761	-0.09	9.3457	2.82

The associated mode shapes ψ_1, ψ_2, and ψ_3 are sine waves of one, two and three half waves, respectively.

Simulating this same simply supported beam by a set of equal lumped masses spaced equidistant along the beam establishes a discrete system which may be solved in any number of different ways. Trial cases have been analyzed using 10, 20, and 30 lumped masses. Comparison of the resultant natural frequencies can be seen in Table 2.

The accuracy of the solution of the discrete system varies with the number of degrees of freedom given to it; note, however, that the relationship is not direct; the accuracy requirements of the task influence the decision as to how many degrees of freedom can be justifiably assigned to the model.

Table 2. Frequency Comparison

Exact Solution and Discrete System Solution for Simply Supported Uniform Beam

System / Mode Number	Continuous (Exact Solution)	10-mass lumped parameter	20-mass lumped parameter	30-mass lumped parameter
1	9.58	9.58	9.58	9.58
2	38.34	38.33	38.34	38.34
3	86.26	86.20	86.26	86.26

(Frequencies are in cycles per second.)

Application of the lumped parameter techniques to space vehicle systems has been used extensively by the aerospace industry. Invariably, the propellant tanks and all cylindrical structures are described as beams with propellant and structural mass distributed. Local stiffnesses are represented as equivalent translational and rotational springs or by experimentally or analytically determined influence coefficient matrices.

There have been several attempts to verify the dynamic characteristics of a launch vehicle as indicated by the analytical model with those obtained by test on the prototype itself. A comparison of experimental and analytical modes for an Atlas with a long, slender payload is given in Reference 2. These results show that frequencies for the first four modes are within 10% accuracy. The mode shapes are fairly well represented in the first four bending modes although displacement amplitudes were found to increase in error with mode number. Using the generalized mass as a measure of mode displacement error these are 4%, 28.2%, 177%, and 20% for the first 4 modes. The fifth mode shape was not well represented although frequency comparison was within 15%.

A similar comparison was made for the Minuteman solid ICBM in Reference 3. These results give a 13% difference for frequency in the first four modes and slightly larger errors in mode shape. After a correction for adapter joint flexibility the maximum error in frequency of the first four modes was 6% with corresponding improvement in mode shape.

Vibration test results of an Atlas-Agena-OAO vehicle, which is a more complex structure than the previously mentioned vehicles, are presented in Reference 4. Here, the first mode compares reasonably well with the analytical modes; however, the higher modes were not representative of the analytical modes. Detailed examination of local structure revealed possible amplitude dependent component stiffnesses. When this characteristic was taken into consideration, the comparison between analytical and test mode shapes was improved to a satisfactory level.

Several important factors can be obtained from the results of these comparisons: (1) the idealization of the tank as a one-dimensional beam appears to be adequate; (2) much attention should be focused on local structure such as connections; (3) the numerical procedures presently available are capable of solving for the primary modes. These studies also verify what might be inferred from the mathematical characteristics: just as the eigenvalues (frequencies) can be determined with greater accuracy than the eigenvectors (mode shapes), so are the frequencies of the physical system more accurately predicted analytically than the corresponding mode shapes. Furthermore, with the numerical methods used to analyze large systems, the accuracy of the calculated characteristics decreases with increasing order of mode number. The redeeming feature is the fact that for most vehicles the overwhelming fraction of response is obtained from the first and sometimes second mode. Consequently, although a sizeable error may be introduced in the higher modes, the net error in total vehicle response is small. As a matter of fact, in the case of cylindrical vehicles, attempts to verify the mathematical representation in flight has succeeded in only identifying the first mode and second mode frequencies from the flight data.

Analysis of clustered boosters is still in the formative stage, although much improved over the earliest attempts at analysis. The first efforts (Reference 5) attempted single beam models, but when tests on the vehicle were performed, the total inadequacies of the single beam analogy were made apparent. It was evident that multidimensional motion and individual tank motions must be defined analytically. The analysis procedure was revised to provide for such motions. The first attempts at such analysis produced results which were still significantly at variance with test data. The primary cause was found in the evaluation of the stiffness of the complex structure. As structural definition improved, so did the modal data. Mathematical difficulties imposed by excessive numbers of coordinates have been overcome by use of the modal synthesis technique (Section 4.3). Modal data thus obtained compares well with both static and flight test data.

In the case of Saturn, the frequency comparison between analysis and test is quite good, (Reference 6). Again the mode shapes do not agree as well, especially in the motion of peripheral tanks. The effect of these modal discrepancies on control and loads is not important. Techniques have been developed whereby these discrepancies are accounted for and reworked as they appear. These discrepancies also vary from one vehicle to another, which sometimes necessitates additional work to obtain satisfactory agreement between model and test.

A variance with cylindrical tank vehicle experience is the composition of flight test response data of clustered tank vehicles. Such data from gyro and accelerometer traces indicates measurable contributions to vehicle response from several bending modes and higher complex modes. (See Reference 7).

3/MODEL REQUIREMENTS AND RECOMMENDED PROCEDURES

The solution of dynamics problems is approached by developing a set of governing equations through consideration of the condition of dynamic equilibrium or of energy relationships of the system under applied external forces. For an undamped system the general form of these equations, in matrix notation, is

$$[M]\{\ddot{z}\} + [K]\{z\} = \{F\} \tag{1}$$

where $[M]$ is a matrix of masses, $[K]$ is a stiffness matrix, $\{z\}$ and $\{\ddot{z}\}$ are the displacement and acceleration vectors, respectively, and $\{F\}$ is a vector of external forces.

A very useful characteristic of elastic systems is that they will respond or vibrate in natural orthogonal modes of displacement ψ_n with circular frequencies ω_n. The total displacement of a system can then be expressed as a summation of individual natural mode displacements. This is given by

$$\{z\} = [\Phi]\{q\} \tag{2}$$

where $[\Phi]$ is a matrix of mode shapes and q_n is the time dependent amplitude of mode n. Substituting equation (2) into equation (1) yields

$$[M][\Phi]\{\ddot{q}\} + [K][\Phi]\{q\} = \{F\}. \tag{3}$$

Premultiplying both sides of (3) by $[\Phi]'$ gives

$$[\Phi]'[M][\Phi]\{\ddot{q}\} + [\Phi]'[K][\Phi]\{q\} = [\Phi]'\{F\}. \tag{4}$$

the requirements of orthogonality and harmonic motion of the natural modes provide the relationships

$$[\Phi]'[M][\Phi] = [m] \tag{5}$$

and

$$[\Phi]'[K][\Phi] = [\omega^2][m]. \tag{6}$$

Substituting (5) and (6) into (4), we obtain

$$\{\ddot{q}\} + [\omega^2]\{q\} = [m]^{-1}[\Phi]'\{F\} = [m]^{-1}\{Q\}. \tag{7}$$

Equation (7) is a set of n uncoupled equations in terms of q_n, ω_n, the generalized mass, m_n and the generalized force Q_n. The solutions of these equations identify the time dependent values of q_n which are then used in equation (2) to give complete system response. Detailed discussions, derivations, and proofs of the equations of motion, orthogonality of natural modes, and normal mode theory are given in References 8 to 11.

The use of normal mode theory requires determination of these natural modes of vibration. If harmonic motion is assumed and the applied forces are equal to zero, then equation (1) can be written as

$$- \omega^2 [M] \{z\} + [K] \{z\} = 0$$

or

$$\{z\} = \omega^2 [K]^{-1} [M] \{z\}. \tag{8}$$

Each of these equations is in a form suitable for solutions to obtain the orthogonal modes and their natural frequencies. Many numerical techniques have been developed to obtain these characteristics and several are discussed in Section 4.2.

The above discussion presents the fundamental approach to structural dynamic response analyses. The mathematical model used to simulate the physical system is the basis for determining the natural modes and the solution of the dynamic problem. It is significant, therefore, to examine in detail the factors influencing its development.

3.1 LATERAL REPRESENTATION OF CYLINDRICAL LIQUID PROPELLANT VEHICLE. In most instances, the lateral dynamic characteristics of liquid rocket propelled space vehicle systems can be considered to be adequately represented by simple one-dimensional beam theory. It is common practice, and certainly more convenient, to replace the continuous structure by a lumped parameter idealization. In such an idealization, the analyst concentrates attention on those aspects of the system which are felt to be dominant (major masses, major structural elements, propellants). The discrete model is formed by concentrating mass at selected points along the beam. These points are ideally the c.g. of the distributed mass which is to be considered concentrated at that point.

Elastic properties are expressed in lumped fashion as a set of flexibility coefficients, C_{ij}, or stiffness influence coefficients, K_{ij}. These coefficients have a physical significance in that C_{ij} can be considered as the deflection of point i due to a unit load at j; and K_{ij} equated to the force produced at point i due to a unit deflection at point j, if all coordinates other than j are temporarily restrained. (Flexibility and

stiffness influence coeff cients are covered in more detail in Section 4.1).

The mathematical description of this discrete model is a set of simultaneous linear ordinary differential equations. Such equations lend themselves readily to matrix techniques and the utilization of digital computers permits the solutions of sets of equations too large for practical hand computation.

The one-dimensional beam representation is the simplest lateral model and may not fulfill all necessary requirements for a specific problem. This can necessitate recognition of non-structural modes (sloshing), local response characteristics (engines) or multiple load paths not accounted for in the simple beam analogy. A further refinement of the model is then necessary.

3.1.1 MASS AND ROTARY INERTIA. The distributed mass and inertia data must be lumped into discrete, point masses, the number of which determine the degrees of freedom given to the model. The number of mass stations is influenced by the number of bending modes to be calculated.

It has been found that for one-dimensional beam bending models the required number of mass stations should be approximately ten times the number corresponding to the highest elastic bending mode to be calculated. For example, if three elastic bending modes are to be calculated, then approximately thirty mass stations are required to represent adequately the bending dynamics of the third mode. This criterion has been established empirically by calculating mode shape, frequency, and generalized mass corresponding to the first three elastic bending modes for typical vehicles configurations in which the numbers of mass stations used were successively increased from eighteen to forty. As expected, the accuracy increased as additional stations were utilized. However, it was observed that no further significant increase in accuracy was achieved by using more than thirty mass stations.

For a more complex model (such as one with branched beams) the above general rule may not be strictly applicable. For a branched system, the general rule may be applied to the primary beam of the system, and masses lumped on the secondary branches in about the same distribution. It must be emphasized that as the model diverges from the single beam concept, performed mass lumping rules become less applicable and more reliance must be placed upon the experience of the analyist.

Note that only rigid masses are to be included in this distribution, that is, only those masses which can be considered to act as an integral part of the unrestrained beam during its vibrations. It cannot be over-emphasized that items such as pumps, equipment pods, etc., which are actually, or simulated as, mounted elastically to the main structure may significantly alter the bending characteristics of the higher frequency modes.

Whether or not such masses are to be treated as integral to the beam or as separate, elastically attached masses, depends upon: (1) whether or not the frequencies of the body modes to be computed are less than or greater than the mount frequencies of the discrete masses, and (2) whether or not these masses are great enough to materially affect the result.

Accurate representation of the distributed mass at discrete points would require inclusion of the mass moment of inertia of the distributed mass at that point. With liquid propellant, the effective moment of inertia is not easily determined. Fortunately, these rotary inertias have only a small influence on the modal quantities of the first two bending modes and can be neglected as shown in the work of Reference 12. 12. This work is a comparison of modal parameters for a typical launch vehicle for calculations with and without rotary inertia terms. (Rotary inertia was calculated assuming the liquid behaved as a solid). The differences in the first two modes were less than 10% for all parameters and less than 5% for most parameters. In the third and fourth modes the differences were usually less than 20% with a few extreme differences up to 100%. These calculations are at the extremes of effective rotary inertia and the correct solution is probably somewhere between. A better representation could be obtained by using more mass stations rather than including rotary inertia.

Because of the small effect in the lower bending modes and the uncertainty of effective inertia, it has been common practice to neglect this term. Also, this allows for much more efficient computation since this eliminates half the coordinates in the solution of characteristic equations.

3.1.2 SLOSHING PROPELLANTS. Space vehicle system propellants constitute a large percentage of the total system weight. Part of this propellant can be considered as rigid or distributed mass on the idealized beam while a smaller portion must be allowed to slosh in the lateral model. This sloshing mass becomes more important in later flight times, when the sloshing mass becomes a sizeable proportion of total vehicle weight. The complex problem of control system coupling with multi-tank slosh masses precludes any simple rule of thumb criteria for sloshing stability. Experiences with some vehicles indicate major instability periods occur when the sloshing masses approach 20% of total vehicle mass.

Several methods have been developed for the description of propellant sloshing modes and frequencies. The general approach, as related to lateral models, is to derive the hydrodynamic equations into a form suitable for a mechanical analogy. It can be shown for a cylindrical tank that if: (1) the tank walls are rigid, (2) the fluid is incompressible and irrotational, and (3) only small disturbances are admitted, then pendulum or spring mass analogies can be devised which will reproduce the characteristics of the fundamental mode of sloshing oscillation. Attaching the equivalent spring-mass to the lateral model is easily accomplished and is therefore preferred over the pendulum. The second and higher sloshing modes are not generally considered because the magnitude of lateral force contribution from these modes decreases rapidly with increasing order; furthermore, test experience indicates a great deal of turbulent mixing occurs and damping effects are greater in higher modes.

Techniques for deriving the mechanical analogies for slosh and their limitations are the subject of another monograph.

3.1.3 ENGINE REPRESENTATION. Thrust-vector control of liquid-propellant vehicles is generally maintained by gimballing the rocket engines. Since the entire engine is gimballed rather than just the thrust vector, this gimballing action will cause inertial forces as well as thrust forces to act on the missile body. These inertial forces are appreciable, and their lateral components will equal those of the thrust forces when the engine is gimballed sinusoidally at a particular frequency; at higher frequencies they can exceed thrust forces. The thrust vector displacement is determined by two effects (1) the displacement contained within the elastic mode (including the flexibility of the engine mounting and actuator structure) while the servo positioning system is locked and (2) the additional degree of rotational freedom added to represent the motion accompanying action of the positioning servo. For an adequate representation in an analysis including the engine and control systems it is necessary to include engine characteristics in the lateral model. The only exception arises when the model frequencies are well below those of the engine mounting system.

The engine is incorporated into the lateral model by attaching a mass and moment of inertia at the appropriate location on the one-dimensional beam. Since the engine itself is quite rigid, the only elasticity normally considered is the mounting structure and actuator system. This structure is generally complex and test data is often required for proper simulation. One such test would be a vibration test to determine the resonant frequency of the engine on its mounts and using these results obtain the equivalent rotational spring connecting the engine to the vehicle. This primary frequency is often low enough to fall within the range of the lower vehicle bending frequencies and as a result could have a significant effect on bending stability.

Other means of obtaining thrust vector control are used and require engine representation in the lateral model. Vehicles using a combination of fixed and gimballing or swivel engines require simulation of the fixed engines as well as the engines with freedom to represent their displacement in the vehicle elastic modes. Control concepts such as movable nozzles or stream deflection, involve little or no additional mass motion and, therefore, only the fixed engine representation would have a significant effect on the lateral modes.

3.1.4 BRANCH BEAMS. Frequently, the vehicle construction will be such that major portions are cantilevered within another structure or are connected through different load paths. Examples are: payloads enveloped by protective fairings, engine compartments of upper stage vehicles suspended in the inter-stage adapter well, or multi-engine vehicles having independent load paths for each engine - such as a center engine supported on the tank cone and peripheral engines mounted to the cylindrical structure of the vehicle.

Such conditions are illustrated in Figure 1. Realistic representations of these arrangements are required, not only for true definition of gross vehicle response, but also to investigate possible interference between parts. These multiple paths can be accounted for by appropriate branch beams from the major planar beam. So long as the analysis is restrained to one dimensional motion, there is no significant added complexity introduced by the branch beams since the compatibility relationships at the junction

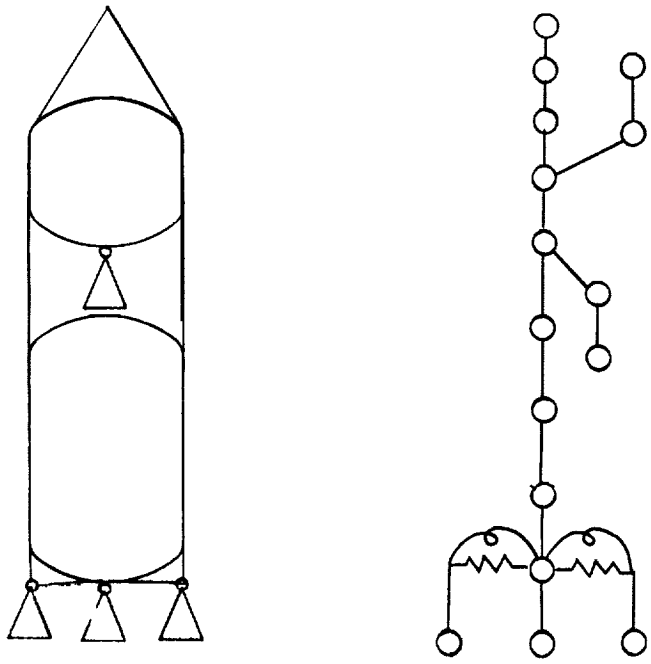

Figure 1. Example of Branched System

points can be easily satisfied. Note the model in Figure 1. Branch beams can be attached in two ways: by secondary beam elements, as is done for the payload fairing and the upper stage engine structure; or by concentrating elasticity in lateral linear and angular springs, as is done for the external engines of the booster. The only mathematical consideration involving in choosing which analogy is more appropriate is that the beam element will influence more elements of the flexibility (or stiffness) matrix than springs will, due to the off diagonal cross-coupling terms.

Generally, these branch beam conditions are encountered with relatively small masses and do not alter the gross vehicle modes significantly except that an additional mode is accounted for where the two branches are out of phase but at nearly the same frequency as the in phase mode. When these branch beams involve engine displacements, they can be significant for control and stability analyses. For other portions of the vehicle they should be included to obtain proper load distribution and clearance envelopes.

3.1.5 LOCAL STRUCTURE EFFECTS. One of the major difficulties encountered in describing a vehicle is the effect of local structures such as joints between the interstage adapters and vehicle stages, trusses on which payload or engines are mounted, or play in joints such as engine gimbal blocks when the engine is not under thrust. In the case of an adapter joint, its stiffness may vary under compression or tension. Although these joints are usually in compression, it is possible during the period of maximum aerodynamic loading for the combination of axial and bending loads to cause one side of the cylinder to be in tension. Depending on the characteristics of the joint, this could lead to a significant error in frequency and mode shape. The variation in stiffness of the joint under these conditions is difficult to determine accurately by analysis and usually test verification is necessary to determine the significance of this effect. Once these values are obtained, they can be substituted in the model and used for the modal calculations.

Similar problems can exist for the local structure supporting engines or payloads since these structures are often redundant, carrying loads to a flexible shell. It is possible to obtain these influence coefficients analytically, but a final check with test results is advisable. The free play occasionally found in connections such as an upper stage engine gimbal (when not under thrust) during first stage flight is random and difficult to represent. These can produce some low frequency pendulum or inverted pendulum modes of significance if the mass involved is appreciable. To determine such effects some crude pendulum-spring mass analogies can be used to establish whether or not further consideration is necessary.

The above are a few local effects to be examined in construction of the lateral model. In general, joints that carry significant loads or components of sizeable mass should be examined in some detail to establish the degree of representation required in the lateral model.

3.1.6 LOCAL NON-LINEARITIES. If major non-linearities exist, the system and its response cannot be described correctly with conventional normal mode analysis techniques. The effect of a separation joint possessing non-linear bending stiffness was investigated through the use of quasi-normal modes and a Rayleigh - Ritz analysis in the work of Reference 12. In the analysis, the assumed mode shapes are those of the vehicle having an infinitely stiff separation joint plus one additional mode having a single concentrated non-linear rotational spring located at the separation point with the remainder of the vehicle considered as rigid. The LaGrange equations produced simultaneous equations in the normal mode coordinates with inertial coupling between the orthogonal elastic modes and the non-linear spring mode.

To the equations of motion developed with the above techniques were added the control sensors, engine representation, and control system representation for a bending stability analysis. Because of the non-linearities in both the vehicle structure and the engine actuators the solution was obtained with an analog computer. The study presents an approach for solving problems in structures with non-linearities using models modified to account for local peculiarities.

3.1.7 TEMPERATURE. Space vehicle systems primary structure are subjected to change in temperature of hundreds of degrees varying from cryogenic temperature to the extreme elevated temperature resulting from aerodynamic heating. This increase in temperature causes a reduction in the material moduli which in turn leads to a small reduction in frequencies and altered mode shapes. Temperature considerations are unimportant until after the period of maximum aerodynamic pressure and then only for certain portions of the vehicle. Since the period of maximum heating occurs after the period of maximum disturbance and only affects parts of the structure, its significance is greatly reduced. The heating of various portions of the vehicle can be predicted within tolerances necessary for modal analyses to establish the resultant variation in modal parameters. It is a condition which should be examined if bending stability is marginal.

3.1.8 AXIAL LOAD. Axial loads caused by longitudinal acceleration of several g's during flight will cause a slight decrease in bending mode frequency through two mechanisms: (1) the effect of axial load on beam vibration, and (2) the reduction in equivalent skin on stringer-skin structure. The first effect can be represented analytically and the second can be included after calculating or obtaining the equivalent skin from empirical data. The total effect of axial loads is generally very small and in nearly all cases can be ignored. In cases where the control system is marginally stable this is one of the several minor effects that must be evaluated. The study in Reference 13 shows that the effect on frequency for representative booster structure is less than 1% when shear stresses are small.

3.1.9 LATERAL-TORSIONAL-LONGITUDINAL COUPLING. The typical axis symmetric cylindrical space vehicle is analyzed as if lateral, torsional, and longitudinal motion are not coupled. Actually, these vehicles are not completely symmetric and a possible coupling mechanism, however slight, can always be found. The importance of this coupling can vary greatly from vehicle to vehicle and even if it is known to exist from flight or experimental data, the coupling mechanism is difficult to identify. These coupling problems often occur when the modal frequencies of two modes, say, one lateral and one torsional, are very close together. Then a very small coupling mechanism, such as c.g. offset from the supposed line of symmetry, can result in coupled motion.

A comparions of the frequencies of the modes in the three directions should be made to determine the existence of modes of nearly equal frequency. If such a condition exists, it is necessary to examine the condition under which this may cause a significant problem. As an example, if a limit cycle can occur due to sloshing, could this cause excitation of a critical torsional mode at this same frequency or sub-harmonic? In most instances of coupling of this type, a periodic forcing function is necessary to transmit the energy from one direction to another.

Cylindrical vehicles with unsymmetric upper stages or payloads of large mass can cause coupling in the various directions in the low frequency modes. The model (and analysis) then become complicated and approaches that of the clustered boosters. Representation of this configuration requires detailed description in the unsymmetric stages and proceeding with analysis as described later for clustered boosters. Preliminary work would indicate the degree of sophistication to be used for adequate representation for stability and loads analysis.

3.1.10 DAMPING EFFECTS. Structural dissipative (damping) forces exist in the vibrating structure as a result of material strain hysteresis and coulomb friction in structural joints. The nature of these damping effects is obscure and does not lend itself to analysis other than an approximate empirical treatment, by which the gross effect of these scattered dissipative mechanisms is represented as an equivalent viscous damping, added to each mode as appropriate. The damping is thus assumed to produce no coupling between modes. While this mechanization is not entirely realistic, it is justified by the following observations:

a. The actual damping is very low and is found by test to produce little coupling. Thus, nearly pure normal modes of a system may be excited and the system observed to decay almost harmonically. The indication given is that velocity dependent coupling is very small.

b. If an attempt is made to show a velocity dependent coupling, the coefficient would have to be determined experimentally. Since the direct damping coefficient is itself difficult enough to measure it is clear that the accuracy of a study can not be increased by the introduction of still more suspect data.

The structural damping force is a function of the deflection of the generalized coordinate of the mode but in phase with the velocity of the generalized coordinate of that mode. To treat this damping as a viscous damping requires that the mode oscillate in a quasi-harmonic manner. This damping force may then be expressed as a damping factor, ξ_n, where $2\xi_n \omega_n \dot{q}_n$ is the internal damping force of the nth mode per unit generalized mass.

Fluid propellant damping forces result from the dissipative nature of a viscous fluid undergoing shear. Although there are some approximate methods for calculating damping forces, these forces are most commonly arrived at by experimental testing of the actual tank, in the case of small missiles, and a model tank in the case of large missiles. These forces may be represented as a propellant damping factor, ξ_l , in the expression $2\xi_l\omega_l\dot{q}_l$ which is the damping force per unit sloshing mass and $\dot{q}_l$ is the lateral velocity of the lth sloshing mass.

Equation (7), with damping included, becomes

$$\ddot{q}_n + 2\xi_n\omega_n\dot{q}_n + \omega_n^2 q_n = m_n^{-1} Q_n \qquad (9)$$

Methods for obtaining values of ξ_n from vibration test date are given in the monograph covering that subject. The dissipative forces associated with sloshing are covered in the sloshing model monograph.

3.2 ADDING COMPONENTS USING MODE SYNTHESIS. Frequently it is desirable to make a parameter study to determine the effect on vehicle response resulting from changes in the characteristics of a specific area or component, e.g. a sloshing mass or engine system. Rather than make several analyses of the system changing but a fraction of the parameters each time, the vibration characteristics of the system excluding the specific varying parameter may be calculated, and then modified by coupling the parameter back in through the mode synthesis technique (discussed in Section 4.3).

For reasons developed more fully in Section 4.3, the mode synthesis approach may result in a loss of accuracy. The analysis that considers the most information about the system will be the most accurate. The use of many modes in the mode synthesis technique will give theoretically more accurate results than using a minimum number of modes. This aspect is one which must be handled by discretion born of experience. As an example, in calculating the bending modes with sloshing propellants, three alternatives are available:

1. Include the sloshing mass as an attached spring-mass to the beam in the modes calculation.

2. Assume the sloshing mass is included in the "rigid" propellants for modes calculation. The sloshing is then included through mode synthesis by adding the single spring mass mode and subtracting the sloshing mass effects from the bending modes. This requires both inertial and elastic coupling in the synthesis.

3. Assume the sloshing mass can be eliminated in the "rigid" propellants for modes calculations. The sloshing is then included through mode synthesis by adding the simple spring mass mode. This requires only elastic coupling in the synthesis.

These alternatives are listed in order of accuracy of end results following the general rule stated previously. There are many examples where there would be little if any degradation of accuracy. As an example, consider a vehicle with first bending frequency of 5 cps and first slosh frequency of 1 cps, then the sloshing is essentially uncoupled from the elastic modes. If the slosh frequency were 4 cps, then considerable coupling is possible.

Although sloshing was used as an example, the same is true for any representation of this type, i.e., engines, payloads, sloshing propellants, or any other large component, or specific parameter under investigation.

3.3 CORRECTING MODEL BASED ON TEST RESULTS. The final verification of analytical techniques is a comparison with experimental data. Perfect comparisons are indeed exceptions, since both the analytical model and experimental model are approximations to some extent. The analytical approximations have been discussed. The major experimental approximations are centered around suspension system effects and vehicle modifications required to accommodate the suspension system. No general rule can be made to obtain better agreement between test and analysis. Careful examination of the data and the structure will probably indicate several areas where the representation is inadequate or does not define the test specimen. Possible causes of differences are:

(1) Effects of suspension system on test environment.
(2) Stiffness of joints or trusses.
(3) Assumed planes of symmetry incorrect.
(4) Effect of large components, such as engines.
(5) Experimental modes may be impure, i.e., not orthogonal or include parts of other modes.
(6) Effects of rotary inertia.

The work of Reference 14 presents a method for obtaining the flexibility matrix from experimental mode data. The procedure orthogonalizes the experimental modes, using an analytical mass distribution, and then derives the flexibility matrix of the structure. This method can be useful if complete and accurate experimental data is obtained for a system difficult to model. It can also be used to locate possible discrepancies between analytical and experimental results.

3.4 SOLID BOOSTERS. The solid propellant grain behaves as a visco-elastic solid. This visco-elastic mass must be represented in some manner when the elastic properties of the booster are calculated. The simplest and most straightforward method of accomplishing this is to consider the grain as an inert mass, rigidly attached to the case. This method, while it has several shortcomings, is in wide use and has been found to yield satisfactory results.

The visco-elastic properties of the grain could be used to provide a more comprehensive analysis of the elastic motion. There are several analytic models which adequately describe the dynamic behavior of the visco-elastic solid (Reference 15 or 16). However, it is generally felt that this area of analysis does not need to be considered for study of lateral bending.

There are several reasons why the visco-elastic properties of the solid propellant grain are not used in calculations of the booster elastic properties. First, they are found to be relatively unimportant for booster vehicles having a reasonable slenderness ratio. The grain structure, in response to stress, exhibits a complicated behavior which can be represented as instantaneous elasticity, delayed elasticity, and viscous flow. For small stresses occurring for short times, the properties could be approximated by considering only the range from 500 to 2000 psi at an ambient temperature of 70-80° F. Thus, the contribution to the bending stiffness is quite small compared to that of the vehicle shell, which is commonly referred to as the solid propellant rocket motor case.

A second consideration is the variable nature of the grain properties themselves. The nature of the approximations which can be used for the model to represent the grain would vary depending on the stress level within the grain, frequency of the application of stress, and temperature. The modulus of elasticity is quite temperature-dependent, exhibiting a change of roughly a factor of 10 for every 40 degrees F of change in grain temperature. This property alone makes it cumbersome to describe adequately the solid propellant grain motion. This difficulty in analysis, along with the relative unimportance of the visco-elastic effects on the mode, has prompted most analysts to omit these effects from the model used to describe the lateral elastic motion of the booster. Bending mode tests run by various airframe manufacturers have indicated that these omissions do not affect the adequacy of the calculations. The above should not be taken to imply that the visco-elastic behavior of the solid propellant grain is not important in all problems. It does become quite important under certain conditions, particularly in the analysis of the longitudinal modes.

From this it follows that aspects important for the liquid cylindrical vehicle lateral model are also to be considered for solid boosters. Propellant sloshing, of course, does not exist. Because of the thicker tank walls of solid boosters, the effects of adapter stiffness and joints are more predominant in the lower frequency modes and should be carefully examined.

3.5 CLUSTERED BOOSTERS. One method for obtaining the higher thrust required for large payloads which minimizes some of the penalties in manufacturing costs and fuel slosh forces involved in increasing booster diameter is the use of clustered boosters. For liquid boosters a peripheral ring of propellant tanks is attached to a center tank and the engines are supported on truss members connecting the tanks; for solid boosters the motors are attached to a central solid or liquid booster. These clustered tank designs destroy axial symmetry and also in some cases planes of symmetry. This results in a more complicated lateral model where a number of cylindrical tanks are coupled by their elastic connections and in the worst cases must be allowed freedom in several directions for an adequate description of vehicle modes.

For preliminary design it is sufficient to choose approximate planes of symmetry and analyze the vehicle for bending modes in pitch and yaw planes using branch beams connected to the central core by translational and rotational springs. Simplified torsional and longitudinal models will also suffice at this stage. These simple models can be used to identify possible problem areas (such as relative modal frequencies) and provide design criteria for the connections between tanks. In some cases the vehicle characteristics are not, and sometimes even cannot, be known with sufficient accuracy to justify any consideration of the effects of non-symmetry.

A complete analysis (or test) should be undertaken to describe all the primary modes of the clustered vehicle. This analysis would provide displacement and rotation in two mutually perpendicular planes (preferably principal axis), torsion, and longitudinal motion. The model of the tanks for displacement and rotation in each of the two planes would be very similar to that discussed for the cylindrical booster. Provision must be made to account for the motion of the outer tanks in these two directions due to the torsional displacement of the center tank and the elastic connections. Longitudinal motions of the outer tanks can couple with the bending motion of the center tank; it is also possible that longitudinal motion will couple with lateral and torsional displacement. As an example, consider a cluster arrangement where the connection at the bottom transmits moment, shear, and axial restraints while the connection at the top provides only shear restraint. Then it is possible to find a mode where the external tanks are bending, causing moments and deflections at the connection to the center tank which will result in longitudinal motion of the tank, as well as modes in which the longitudinal motion of the outer tanks cause bending of the center tank. The significance of these types of modes can only be ascertained from the analysis (or test) and can vary greatly from vehicle to vehicle.

The torsional properties in the model can be represented by the torsional stiffness and roll inertia of each tank. The tanks must then be connected by the elastic properties of the truss. Formation of the torsional and longitudinal models are given in the monographs on those subjects. The complete model for the clustered booster then consists of the lateral model in two planes, the torsional model and the longitudinal model. These models are then combined through the elasticity and geometry of the connections to provide the stiffness and/or mass coupling.

Analysis (or test) will probably show some planes of symmetry and can also show that some of the coupling mechanisms are unimportant for the particular problem to

be solved. If this is the case, it is justified, and expedient, to devise a mathematical model from the results of the complete anlysis (or test) which represents the modes of interest.

The analytical representation of the clustered booster is more approximate than that of the one-dimensional beam lateral model, especially for the condition of coupled modes. The tri-axial strain relationships are not completely satisfied, and the inertia terms could be poorly represented in the combination lateral-axial motion. These effects generally are of second order and as such should not alter the primary modes. The elasticity of the connection points probably will require test data for accurate values. The numerical techniques employed for the solution of the system characteristics have been used for many years in the industry; however, some problems in accuracy can be encountered when applied to the clustered booster. The number of points describing the system may be compromised for efficient computer operation and this vehicle may have modes of nearly equal frequency which will be difficult to separate analytically (and experimentally).

The elasticity of the vehicle is most easily described by a coupled stiffness matrix, but solving for the characteristics would then involve inversion of this matrix. This inversion may lead to errors because of machine round-off errors. If the inversion is successful, round-off errors could still be significant in the iterations for the characteristic values, especially for modes with nearly equal eigenvalues. The inversion problem can be circumvented by writing the coupled flexibility matrix directly. The required transformations can be complicated and lead to errors, but with special care this is not insurmountable. Another approach would develop an uncoupled flexibility matrix and perform transformations of coordinates to provide all necessary coupling in the mass terms. These last two approaches would still have possible problems in the iterations on the systems characteristics.

An approach useful in calculating modes of complex systems is the component mode synthesis method. Here the modes of the individual pieces are calculated and then the combined modes are obtained from the modes of the component parts. This is based on the assumption that significant motions of the individual tanks can be described by a small number of modes. If this is true, then the solutions for the combined system can be performed in terms of less coordinates.

Most of the clustered booster work to this date has involved two vehicles - - the Titan IIIC and the Saturn I (and the second generation Saturn 1B). Titan IIIC is comprised of a center core liquid booster with two attached solid boosters (Figure 2); the connections at the bottom transmit axial load, shear, moment, and torque. The top connection transmits only shear. Because of the nature of the connections, it can be seen that yaw bending and longitudinal coupling can occur and pitch bending and torsion is another possible coupling mechanism. Storey in Reference 17, develops the coupled flexibility matrices for these two conditions. This method encountered difficulty in that the number of stations required for adequate representation of the system with the required transformations exceeded computer capacity.

The final Titan IIIC analysis presented in Reference 18 utilizes the mode synthesis approach. The longitudinal, torsional, and pitch and yaw bending modes are determined for each tank and are then coupled by the elasticity of the connecting elements. The influence coefficients for these trusses were obtained experimentally. A report giving comparison of analytical and 1/5 scale experimental results is to be published.

The Saturn I vehicle consists of a center LOX tank with eight peripheral tanks for alternately LOX and RP-1. These tanks are connected at top and bottom by trusses (Figure 3) providing axial, shear, and torsion restraint in both planes at the bottom plus moment restraint in the tangential planes. The top connection provides similar restraint except for the fuel tanks which do not transmit axial load. The trusses are not symmetric with respect to planes of symmetry of the tanks, but this effect is small such that planes of symmetry as defined by the tanks do not introduce large errors.

Kiefling (Reference 6) uses a mode synthesis approach for calculation of Saturn I modes. Pitch, yaw, and torsion are considered uncoupled and the effect of longitudinal propellant vibrations in the outer tanks is coupled with bending. A comparison with test data shows very good agreement in frequency, while agreement of mode shapes is fairly good. The discrepancy, which is seen in the seventh and some higher modes, is in the displacements of the booster center tank. Since no control sensors are located in this area, this discrepancy is of limited importance for stability and control studies. The mode shape differences are due to deflections of the spider beam, the structure connecting the top of the booster tanks and the second stage.

Two higher modes determined analytically were not found during the test. Theoretical response in these modes was very small; therefore, the modes would be difficult to excite.

Milner (Reference 19) establishes theoretically the uncoupling of pitch, yaw, and torsion modes for a symmetrical clustered booster and investigates the effect of minor asymmetry. Results of this study indicate that the effect of such coupling on natural frequencies is minor; mode shapes are not presented.

O'Rourke (Reference 20) applies Kron's method to the analysis of an early Saturn vehicle. Based on a total of 135 mass points, seven modes of the vehicle were found in this analysis. Comparison of these results with dynamic test data is generally as good as can be expected, since the analysis was based entirely upon theoretical stiffness of the very complex structure. The dynamic data (modes) were obtained by a frequency analysis of the vehicle response to a sinusoidal force. It was assumed that the vehicle natural modes existed at points of maximum response.

Bost (Reference 21) analyzes the Saturn vehicle using a composite mode method. Eight modes are found. Agreement with published test data is only fair. Again, the difficulty was of obtaining a structural mathematical model which represents

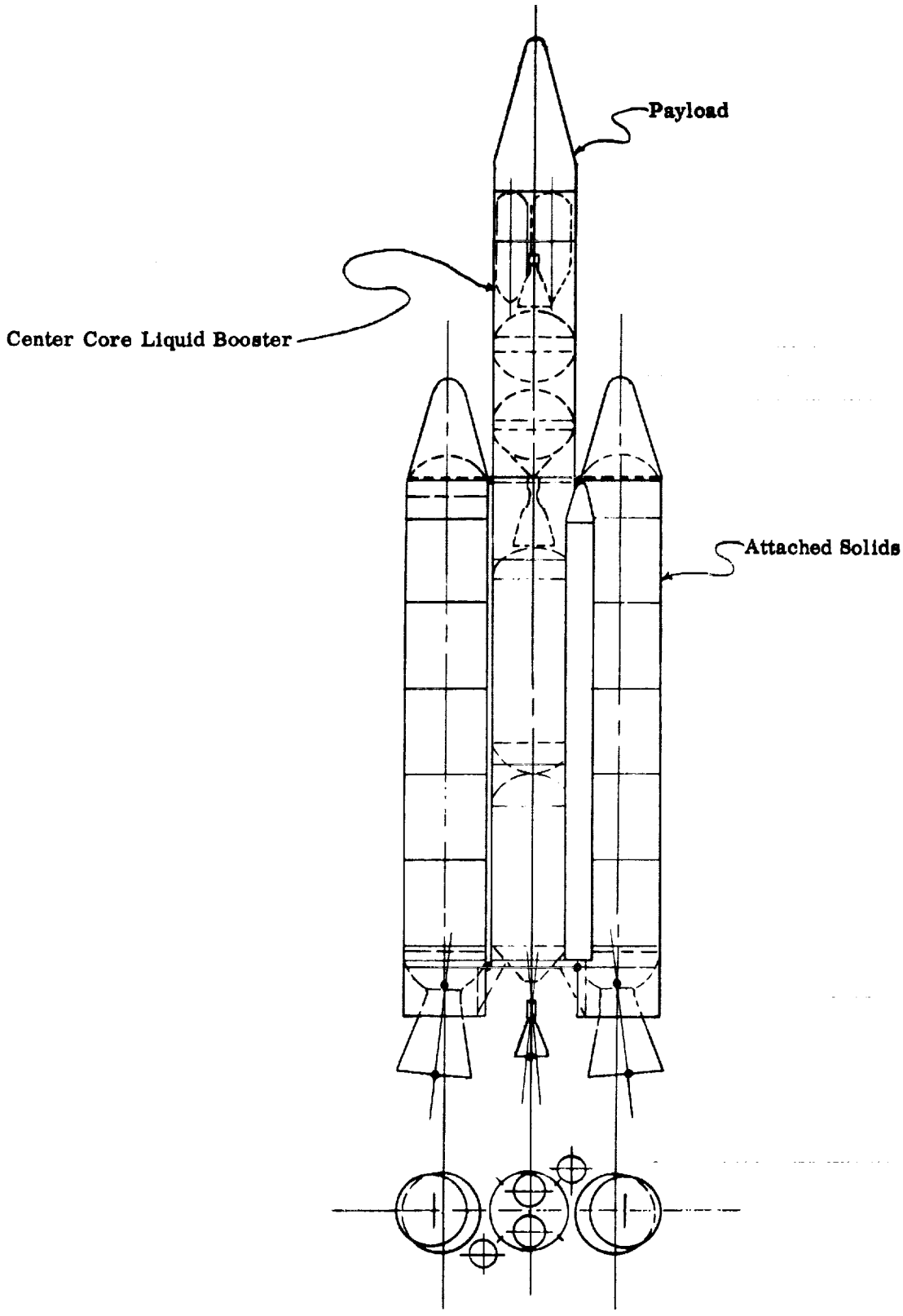

Figure 2. Titan III C

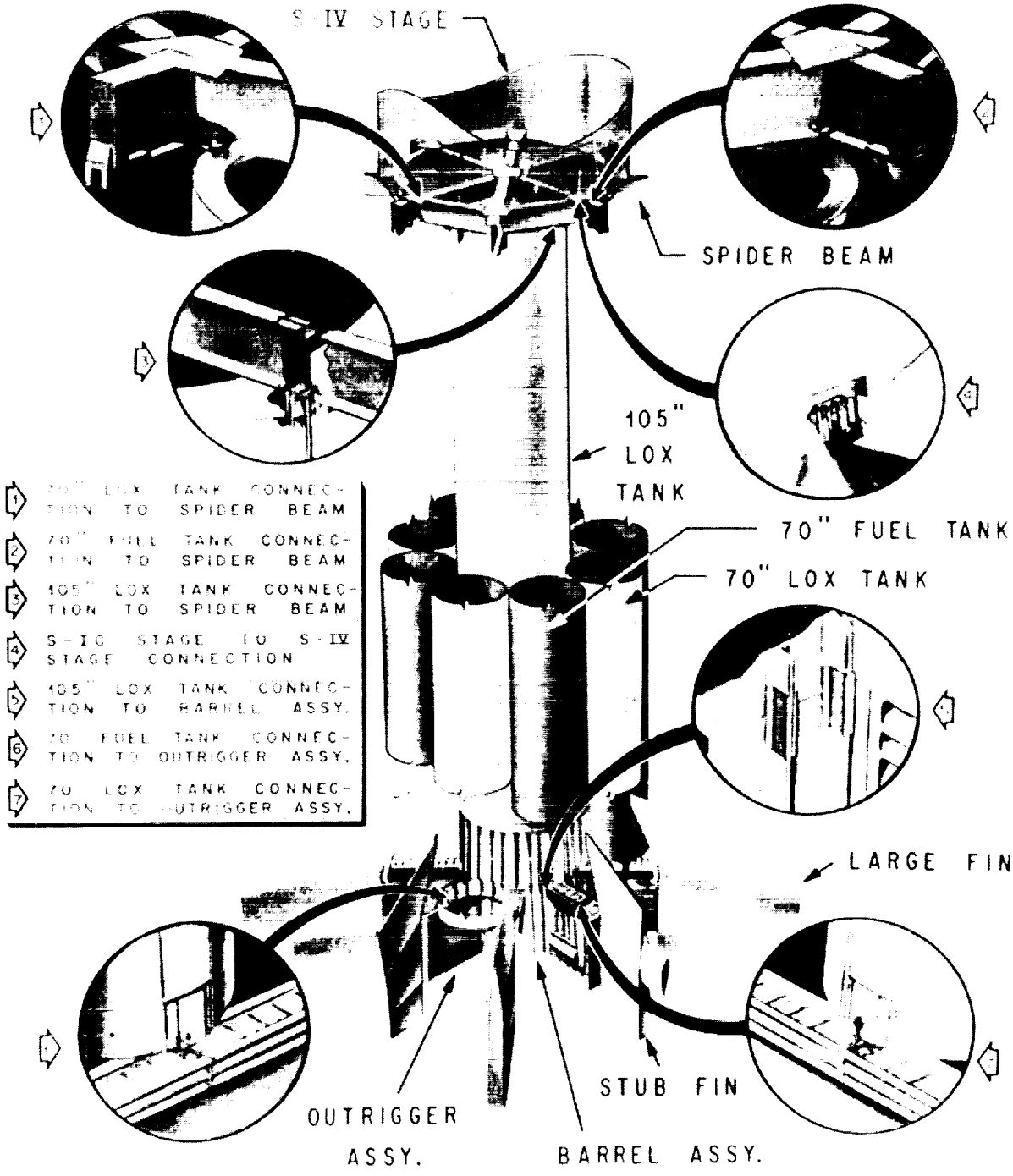

Figure 3. Saturn I Booster Details

adequately the actual vehicle.

Republic Aviation currently is engaged in a Saturn I vibration study using Lanczos' method of minimized iteration (Reference 22) for solution of the eigenvalue problem. The method used for calculating the matrix of influence coefficients is described by Meissner (Reference 23), while the calculation of the dynamic matrix is shown by Berman (Reference 24). The complete method is demonstrated on a simple cluster beam configuration in Reference 25 , in which seven modes and frequencies of a 72 degree of freedom system are determined successfully. Preliminary, unpublished results from the attempted application to a full scale Saturn including sloshing and using 368 degrees of freedom indicate that problems with scaling, round-off errors, and excessive machine time exist for the large number of modes desired.

Whetstone at Lockheed is currently working on an extension of the mode synthesis approach to include the effects of spider beam flexibility, but no data has been published at the present time.

Glaser, (Reference 26), constrains the center tank of Saturn I vehicle to oscillate in a plane of symmetry; the outer tanks are restricted to motions symmetric to this plane. The inner and outer tanks are coupled together through the use of equations of compatibility at the connection points. The solution is carried out by a Myklestad - type analysis. Lowey (Reference 27) also uses a Myklestad approach on a model whose center tank is constrained to move in a single plane; axial motion of the outer tanks is permitted. Results from both these analyses are not available at this time.

Lianis (Reference 28) develops a matrix solution of the dynamics problem of a four tank booster without center core. The flexibility matrix of the whole unit, with appropriate end fixity, is derived. This flexibility matrix together with suitable mass matrix is used to derive equations of free vibration in matrix form. The tanks are assumed to be similar, but the solution can be modified accordingly for the case of non-similar tanks and for other tank configurations. The formulation is general so as to furnish any complex mode of vibration. Simple modes, however, can be obtained as particular cases of the general problem.

4/METHODS FOR SOLUTION

4.1 FORMATION OF COUPLED EQUATIONS

The primary purpose of the lateral model is to obtain a representation of the real system which can then be represented in mathematical terms. The general approach to dynamic problems as given by Equations 1 to 8 requires the formation of the mass, stiffness, and dynamic matrices.

4.1.1 STIFFNESS MATRIX. Formation of Equation 8 requires the mass matrix and the inverse of the stiffness matrix. Since the inverse of the stiffness matrix is the flexibility matrix, one may question a method of analysis beginning with the stiffness matrix when a flexibility matrix can be derived directly. The main advantage of the stiffness approach is the straight forward manner of deriving a coupled matrix which lends itself toward formulation of computer logic capable of assembling a coupled stiffness matrix for very complicated systems. Also, with high speed, accurate computers available, the matrix inversion can usually be accomplished efficiently and accurately. Therefore, it is of interest to derive one general computer program which will develop the stiffness matrix of various complex systems from simple input format and instructions. For certain specific problems it may be desirable to develop the flexibility matrix. In this section the approach (as presented in Reference 29) for developing the stiffness matrix for a lateral model will be given. The flexibility approach is presented in Section 4.1.2 and a mass coupling technique is presented in Section 4.1.3.

Bending and shear stiffness are identified as points along the structure including all mass stations. The nature of the stiffness distributions may justify stiffness definition at an intermediate point between mass concentrations. Thus the model is formed from a series of connected massless beams, with mass and inertia concentrations located at some or all of the junctions of the beams. While the stiffness of the vehicle may be distributed in a complex fashion, it may be represented with acceptable accuracy by a series of straight line segments. This results in giving each beam segment a trapizoidal stiffness distribution.

4.1.1.1 Free Element Stiffness Matrix. In the approach to be outlined, the 4 x 4 stiffness matrix of each element of the beam is first obtained by inverting the 4 x 4 flexibility matrix of this element. (The element stiffness matrices are developed by this technique because it is easier mathematically and more accurate.) The matrix is then coupled by constructing a matrix composed of the individual 4 x 4 matrices. In this

coupled matrix, the terms for common points of adjacent elements are the sum of the terms for the individual matrices. With this matrix form, restraints or boundary conditions are imposed which will represent the system to be analyzed. The derivation of the stiffness matrix is now given.

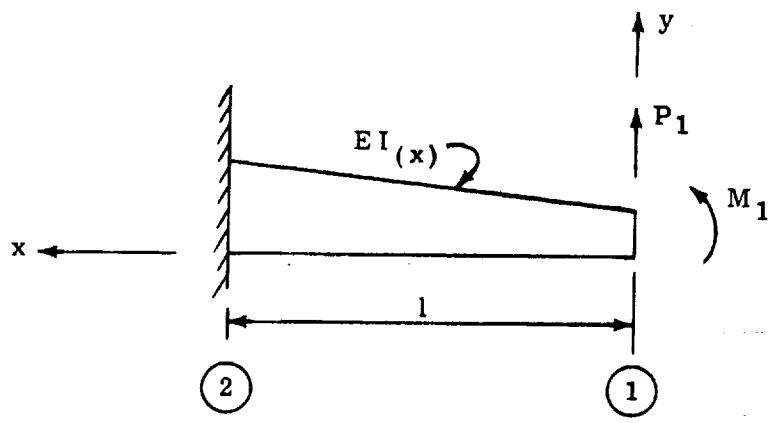

Figure 4. Cantilever Beam in Bending

The bending stiffness for a value of x is

$$(EI)_x = (EI)_1 \left[1 + \frac{x}{l} \left\{ \frac{(EI)_2}{(EI)_1} - 1 \right\} \right]. \tag{10}$$

The general equation of the elastic curve of a deflected beam is

$$\frac{d^2y}{dx^2} = \frac{M}{EI} = \frac{M_1 + P_1 x}{(EI)_x} \quad . \tag{11}$$

Integrating (11) and substituting the boundary conditions $\frac{dy}{dx} = y = 0$ at $x = l$, then y_1 and θ_1, the deflection and negative slope at $x = 0$ are:

$$\left.\begin{aligned} y_1 &= \frac{M_1 l^2}{\bar{a}\,\bar{b}^2} \left[\ln\ (1+\bar{b}) - \bar{b} \right] - \frac{P_1 l^3}{\bar{a}\,\bar{b}^3} \left[\bar{b} - \frac{\bar{b}^2}{2} - \ln\ (1+\bar{b}) \right] \\ \theta_1 &= \frac{M_1 l}{\bar{a}\,\bar{b}} \ln\ (1+\bar{b}) + \frac{P_1 l^2}{\bar{a}\,\bar{b}^2} \left[\bar{b} - \ln\ (1+\bar{b}) \right] \end{aligned}\right\} \tag{12}$$

where $\bar{a} = (EI)_1$ and $\bar{b} = \dfrac{(EI)_2}{(EI)_1} - 1$.

By a similar procedure, the deflection due to shear at x = 0 is

$$\left.\begin{aligned} y_1 &= \frac{P_1 l}{\bar{c}\,\bar{d}} \ln (1+\bar{d}) \\ \theta_1 &= 0 \end{aligned}\right\} \tag{13}$$

where $\bar{c} = (KAG)_1$ and $\bar{d} = \dfrac{(KAG)_2}{(KAG)_1} - 1$.

Putting (12) and (13) into matrix form

$$\begin{Bmatrix} y_1 \\ \theta_1 \end{Bmatrix} = \begin{bmatrix} C_{11} & C_{12} \\ C_{21} & C_{22} \end{bmatrix} \begin{Bmatrix} P_1 \\ M_1 \end{Bmatrix} \tag{14}$$

where C_{11}, C_{12}, C_{22}, are the coefficients of (12) and (13). Then, by inversion,

$$\begin{Bmatrix} P_1 \\ M_1 \end{Bmatrix} = \frac{1}{N} \begin{bmatrix} C_{22} & -C_{12} \\ -C_{21} & C_{11} \end{bmatrix} \begin{Bmatrix} y_1 \\ \theta_1 \end{Bmatrix} \tag{15}$$

where

$$N = C_{11} \quad C_{22} - C_{12}^2 \ .$$

The stiffness matrix is then

$$[K] = \frac{1}{N} \begin{bmatrix} C_{22} & -C_{12} \\ -C_{21} & C_{11} \end{bmatrix} \ . \tag{16}$$

Considering a free element, with the same stiffness as the cantilever beam (as shown in Figure 5), the equilibrium equations are:

$$P_1 + P_2 = 0$$

$$M_1 + P_1 l + M_2 = 0 .$$

Also from Figure 5,

$$y^* = y_1 - y_2 - \theta_2 l$$

$$\theta^* = \theta_1 - \theta_2$$

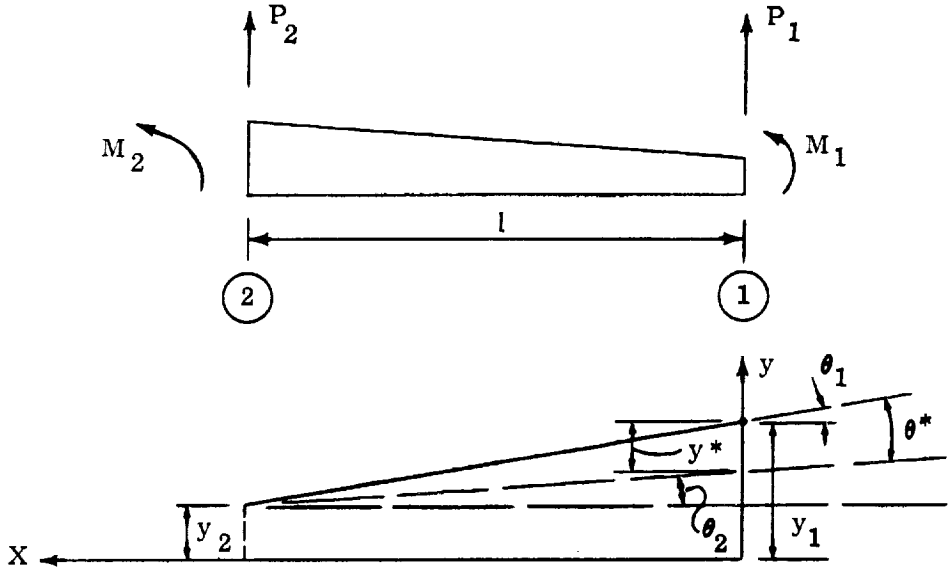

Figure 5. Free Beam in Bending and Shear

Equation (15) now becomes:

$$\begin{Bmatrix} P_1 \\ M_1 \end{Bmatrix} = \frac{1}{N} \begin{bmatrix} C_{22} & -C_{22} & -C_{12} & \left(C_{12} - l C_{22}\right) \\ -C_{12} & C_{12} & C_{11} & \left(l C_{12} - C_{11}\right) \end{bmatrix} \begin{Bmatrix} y_1 \\ y_2 \\ \theta_1 \\ \theta_2 \end{Bmatrix} . \tag{17}$$

Expanding this to include point 2 (by use of the equilibrium equations):

$$\begin{Bmatrix} P_1 \\ P_2 \\ M_1 \\ M_2 \end{Bmatrix} = \frac{1}{N} \begin{bmatrix} C_{22} & -C_{22} & -C_{12} & \left(C_{12} - l C_{22}\right) \\ -C_{22} & C_{22} & C_{12} & \left(l C_{22} - C_{12}\right) \\ -C_{12} & C_{12} & C_{11} & \left(l C_{12} - C_{11}\right) \\ \left(C_{12} - l C_{22}\right) & \left(l C_{22} - C_{12}\right) & \left(l C_{12} - C_{11}\right) & \left(C_{11} - 2l C_{12} + l^2 C_{22}\right) \end{bmatrix} \begin{Bmatrix} y_1 \\ y_2 \\ \theta_1 \\ \theta_2 \end{Bmatrix} \tag{18}$$

The stiffness matrix for a free-free element has been obtained. The nature of the expressions for C_{11}, C_{12}, and C_{22} is such that as EI_2 approaches EI_1, the expressions become indeterminate in form. Each has a limit which is the appropriate coefficient for a beam of uniform cross section:

$$C_{11} = \frac{l^3}{3\bar{a}} + \frac{l}{\bar{c}}$$

$$C_{12} = \frac{l^2}{2\bar{a}}$$

$$C_{22} = \frac{l}{\bar{a}} .$$

It has been found that the use of these values when $|\bar{b}, \bar{d}| < 0.01$ produces little or no error, hence, within this range, it is recommended that uniform beam coefficients be substituted for the original expressions.

4.1.1.2 Axial Load Effects. To determine the effect of axial load on the stiffness matrix of a uniform beam element, consider the model in Figure 6. With an axial compressive force, H, the moment and shear at any section, x, are given by:

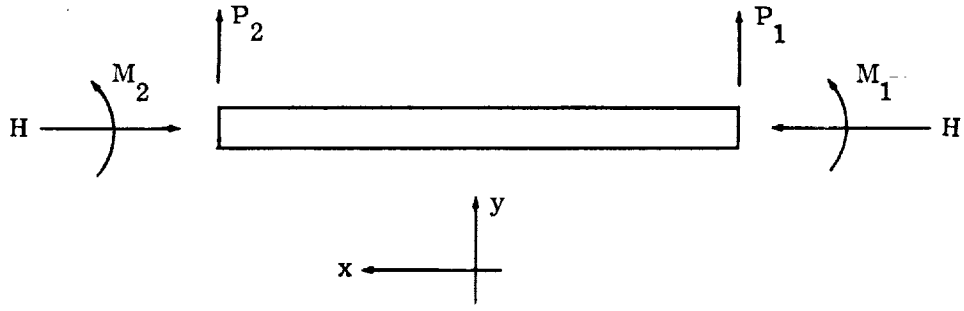

Figure 6. Beam Element with Axial Load

$$\left.\begin{aligned} M &= M_1 + P_1 x + H\left(y_1 - y\right) \\ V &= P_1 - H\frac{dy}{dx} \end{aligned}\right\} \qquad (19)$$

$\frac{dy}{dx} = -\left(\theta + \gamma\right)$ where θ is the slope due to bending and γ is the slope due to shear. Utilizing the relationships $\gamma = V/KAG$ and $\frac{d\theta}{dx} = -\frac{M}{EI}$ the following is obtained:

$$\frac{d^2y}{dx^2} = -\frac{d\theta}{dx}\left[\frac{1}{1-\frac{H}{KAG}}\right] = \frac{M}{EI\left(1-\frac{H}{KAG}\right)} \qquad (20)$$

or substituting from (19)

$$\frac{d^2y}{dx^2} + u^2 y = \frac{M_1 u^2}{H} + \frac{P_1 u^2 x}{H} + u^2 y_1 \qquad (21)$$

where $$u^2 = \frac{H}{EI\left(1 - \frac{H}{KAG}\right)}$$

Integrating (21) and applying the equilibrium equations gives the four deformations y_1, y_2, θ_1 and θ_2 in terms of external forces P_1, P_2, M_1, and M_2. Expressing these relationships in matrix form and inverting gives the symmetric stiffness matrix

$$\begin{Bmatrix} M_1 \\ P_1 \\ M_2 \\ P_2 \end{Bmatrix} \begin{bmatrix} K_{11} & & & \\ K_{21} & K_{22} & & \\ K_{31} & K_{32} & K_{33} & \\ K_{41} & K_{42} & K_{43} & K_{44} \end{bmatrix} \begin{Bmatrix} \theta_1 \\ y_1 \\ \theta_2 \\ y_2 \end{Bmatrix} \quad \text{(sym)} \qquad (22)$$

where

$$K_{11} = \frac{H}{\Gamma}\left[\frac{\sin ul}{u\left(1 - \frac{H}{KAG}\right)} - l\cos ul\right] = K_{33}$$

$$K_{21} = \frac{H}{\Gamma}(1 - \cos ul) = -K_{41} = -K_{43} = K_{32}$$

$$K_{22} = \frac{H}{\Gamma}\left[u\left(1 - \frac{H}{KAG}\right)\sin ul\right] = K_{44} = -K_{42}$$

$$K_{31} = \frac{H}{\Gamma}\left[1 - \frac{\sin ul}{u\left(1 - \frac{H}{KAG}\right)}\right]$$

and

$$\Gamma = 2(1 - \cos ul) - ul\left(1 - \frac{H}{KAG}\right)\sin ul\ .$$

The above matrix is good only for a positive (compressive) load. If the load were negative, u would be the square root of a negative number. Therefore, another derivation is needed to obtain a stiffness matrix for negative (tension) loads. The derivation is the same except that the sign of H is changed and

$$v^2 = \frac{H}{EI\left(1 + \frac{H}{KAG}\right)}$$

is used in place of u^2. As a result, the elements of the stiffness matrix become

$$k_{11} = \frac{H}{\Gamma}\left[\frac{\sinh\ vl}{v\left(1 + \frac{H}{KAG}\right)} - l\cosh\ vl\right] = K_{33}$$

$$k_{21} = \frac{H}{\Gamma}\ (\cosh\ vl - 1) = -K_{41} = -K_{43} = K_{32}$$

$$k_{22} = -\frac{H}{\Gamma}\left[v\left(1 + \frac{H}{KAG}\right)\sinh\ vl\right] = K_{44} = -K_{42}$$

$$k_{31} = -\frac{H}{\Gamma}\left[\frac{\sinh\ vl}{v\left(1 + \frac{H}{KAG}\right)} - l\right]$$

where

$$\Gamma = -\left[2\ (1 - \cosh\ vl) + vl\left(1 + \frac{H}{KAG}\right)\sinh\ vl\right].$$

4.1.1.3 Local Effects. Locally significant components can generally be included in the model by attaching a mass and/or inertia at the appropriate location by means of springs representing the elasticity of the mounting structure. The stiffness matrices of elements representing translational and rotational springs of Figure 7 can be written directly as:

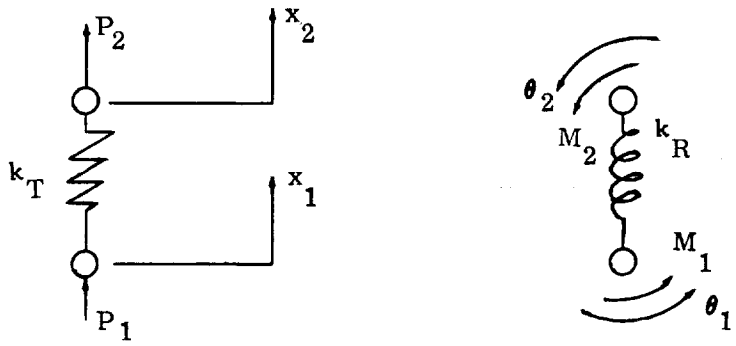

Figure 7. Translational and Rotational Springs

$$\begin{Bmatrix} P_1 \\ P_2 \end{Bmatrix} = \begin{bmatrix} k_T & -k_T \\ -k_T & k_T \end{bmatrix} \begin{Bmatrix} x_1 \\ x_2 \end{Bmatrix} \tag{23}$$

$$\begin{Bmatrix} M_1 \\ M_2 \end{Bmatrix} = \begin{bmatrix} k_R & -k_R \\ -k_R & k_R \end{bmatrix} \begin{Bmatrix} \theta_1 \\ \theta_2 \end{Bmatrix} . \tag{24}$$

4.1.1.4 Coupled Unrestrained Stiffness Matrix. The unrestrained stiffness matrix is generated from each beam element, and a 2 x 2 stiffness matrix is generated from each spring element.

Consider a beam element. If an element is attached to a beam, this element must either be another beam or a spring, Figure 8.

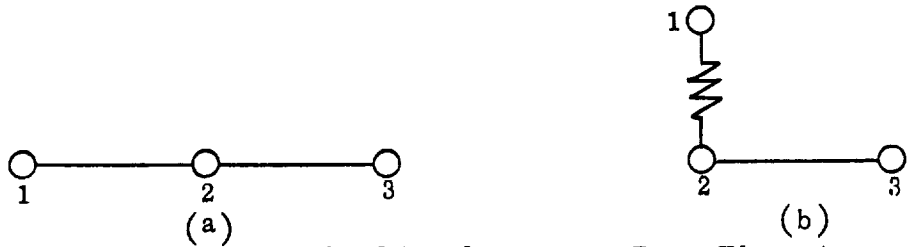

Figure 8. Example of Attachments to a Beam Element

When two beam elements are connected to the same node, coupling with respect to both translation and rotation occurs.

The stiffness matrix layout corresponding to Figure 8 a is given in Figure 9. An element in the matrix of Figure 9 gives the magnitude of the force P_i or moment M_i at node i due to a unit deflection y_j or slope θ_j at node j. Notice that the two beam stiffness matrices overlap at node 2, indicating node 2 feels the effect of both beams. An element in this portion of the matrix is obtained by adding the corresponding element of the two individual stiffness matrices.

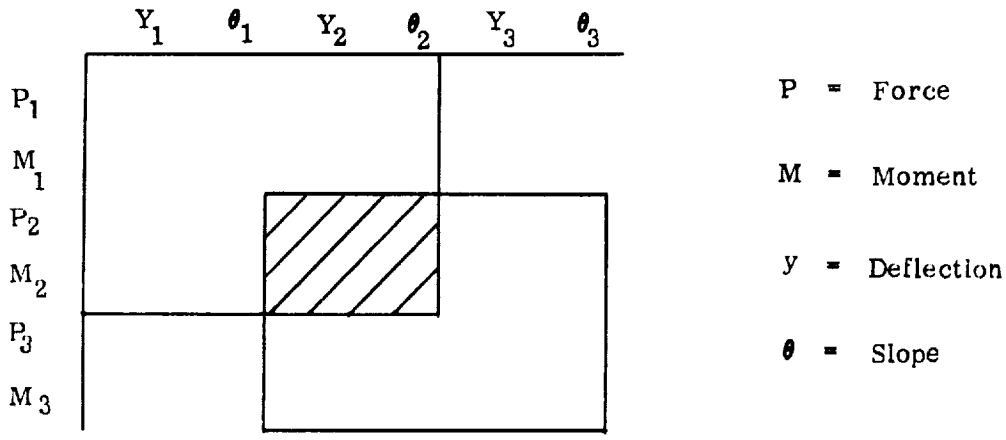

Figure 9. Stiffness Matrix Layout for Attachment of Two Beams

The stiffness matrix layout corresponding to Figure 8 b is given in Figure 10. The two stiffness matrices again overlap at node 2, but this time at one element. Coupling a beam with a spring only affects one degree of freedom, for a spring can have but one degree of freedom. (If instead of a translational spring connected at node 2, a rotational spring were connected, then coupling would be at element M_2, θ_2.)

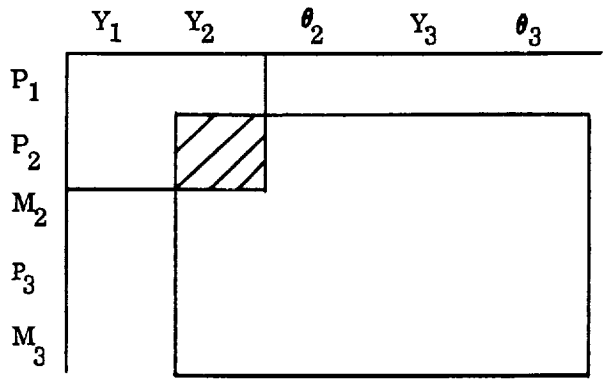

Figure 10. Stiffness Matrix Layout for Attachment of Beam with a Spring

4.1.1.5 Reducing the Stiffness Matrix. The stiffness matrix, as developed in the preceding may contain coordinates which can be eliminated by consideration of the restraints put on a system and the application of boundary conditions to the system. Together, the restraints and boundary conditions can be considered to be in two classes. These are:

a. Nodes that have zero generalized displacements but may have non-zero generalized forces.

b. Nodes that have zero generalized forces (no mass or inertia) but may have non-zero generalized displacements.

The equation $\{P\} = [K]\{y\}$ may be rearranged as follows:

$$\left\{\begin{array}{c} P_s \\ M_s \\ \hline P_o \\ M_o \end{array}\right\} = \left[\begin{array}{c|c} a & b \\ \hline b' & c \end{array}\right] \left\{\begin{array}{c} \phi_s \\ \alpha_s \\ \hline \phi_o \\ \alpha_o \end{array}\right\} \qquad (25)$$

where the P_s and M_s are forces and moments, respectively, that have the non-zero displacement and slopes ϕ_s and α_s. The P_o and M_o are forces and moments respectively that have the zero displacements and slopes ϕ_o and α_o. If

$$\{F_s\} \equiv \begin{Bmatrix} P_s \\ M_s \end{Bmatrix} \qquad \{R_s\} \equiv \begin{Bmatrix} P_o \\ M_o \end{Bmatrix}$$

and

$$\{\zeta_s\} \equiv \begin{Bmatrix} \phi_s \\ \alpha_s \end{Bmatrix} \qquad \{\rho_s\} \equiv \begin{Bmatrix} \phi_o \\ \alpha_o \end{Bmatrix} \equiv \{0\}$$

then equation (25) becomes

$$\begin{Bmatrix} F_s \\ R_s \end{Bmatrix} = \left[\begin{array}{c|c} a & b \\ \hline b' & c \end{array}\right] \begin{Bmatrix} \zeta_s \\ 0 \end{Bmatrix} . \tag{26}$$

Equation (26) is equivalent to the following two matrix equations

$$\{F_s\} = [a] \{\zeta_s\} \tag{27}$$

and

$$\{R_s\} = [b'] \{\zeta_s\} . \tag{28}$$

If there are no boundary conditions associated with the generalized forces $\{F_s\}$, the matrix $[a]$ is the final stiffness matrix $[K]$ and $\{\zeta_s\}$ is a mode shape $\{\psi\}$. If there are also boundary conditions calling for zero generalized forces then matrix equation (27) is rearranged to become

$$\begin{Bmatrix} F_f \\ R_f \end{Bmatrix} = \left[\begin{array}{c|c} d & e \\ \hline e' & g \end{array}\right] \begin{Bmatrix} \psi_f \\ \rho_f \end{Bmatrix} \tag{29}$$

where the F_f are the non-zero generalized forces that have the generalized displacements ψ_f, and the R_f are the zero generalized forces that have the generalized displacements ρ_f.

Equation (29) is equivalent to the following two matrix equations

$$[d] \quad \{\psi_f\} + [e] \quad \{\rho_f\} = \{F_f\}$$

and

$$[e'] \quad \{\psi_f\} + [g] \quad \{\rho_f\} = \{R_f\} \equiv \{0\} .$$

Therefore,

$$\{\rho_f\} = -[g]^{-1} [e'] \{\psi_f\} \tag{30}$$

and

$$\{F_f\} = \left[[d] - [e] \ [g]^{-1} \ [e']\right] \ \{\psi_f\} \equiv [K] \ \{\psi_f\}. \tag{31}$$

In this case (the case of zero generalized forces) the matrix $\left([d] - [e] \ [g]^{-1} \ [e']\right)$ is the final stiffness matrix $[K]$ and $\{\psi_f\}$ is a mode shape $\{\psi\}$.

4.1.1.6 Elimination of Rigid Body Modes. The foregoing analysis was made for a restrained system, one that is fixed at least in one place. For a structure that is completely free (a free-free system), it can be shown that the eigenvalve problem is one of the form:

$$[C] \quad [M] \quad [\psi] = \lambda \left[\{\psi\} - \{\mu\} \ w_o - \{\tau\} \ \nu_o\right] \tag{32}$$

In the analysis of a free-free system the structure must be fixed temporarily at one point. If the structure were not fixed, an external force or moment applied to the system would cause the whole system to move uniformly. The solution to the problem would then be impossible. Mathematically this is represented by a singular stiffness matrix $[K]$. In Equation (32) the term $- \{\mu\} \ w_o$ releases the fixed point with respect to rranslation, while the term $- \{\tau\} \ \nu_o$ releases the fixed point with respect to rotation.

The translation and rotation imparted to the fixed point when it is released are w_o and ν_o. By applying the principles of linear and angular momentum to the system, equation (32) can be expressed as a standard eigenvalue problem.

$$\left[\; [C] \; [M] + [TT] + [TR] \; \right] \{ \psi \} = \lambda \{ \psi \} \qquad (33)$$

where, as explained in the foregoing

$$[TT] \{ \psi \} \equiv \lambda \{ \mu \} \; w_o \, ,$$

$$[TR] \{ \psi \} \equiv \lambda \{ \tau \} \; \nu_o \, ,$$

and

$$\left[\; [C] \; [M] + [TT] + [TR] \; \right] .$$

is the final dynamic matrix. The derivation of $[TT]$ and $[TR]$ is now given.

Referring to Equation (32):

μ_i = 1.0 if point i has a translation degree of freedom.

μ_i = 0 if point i has a pitching degree of freedom.

τ_i = the perpendicular distance from the pitch axis through point zero (origin) to point i if point i has a translational degree of freedom. (Positive if measured forward of point zero.)

τ_i = 1.0 if point i has a pitch degree of freedom.

Applying the conservation of linear momentum

$$m_o w_o + \{\mu^2\}' [M] \{\psi\} = 0 \tag{34}$$

and the conservation of angular momentum

$$I_{m_o} \nu_o + \{\tau\}' [M] \{\psi\} = 0 \tag{35}$$

Multiplying equation (32) by $\{\mu\}' [M]$ yields

$$\{\mu\}' [M] \{\psi\} - w_o \{\mu\}' [M] \{\mu\} - \nu_o \{\mu\}' [M] \{\tau\}$$

$$= \omega^2 \{\mu\}' [M] [C] [M] \{\psi\} .$$

Defining

$$\lfloor A \rfloor = \{\mu\}' [M] [C] [M]$$

and substituting from equation (34)

$$-m w_o - w_o \{\mu\}' [M] [\mu] - \nu_o \{\mu\}' [M] \{\tau\} = \omega^2 \lfloor A \rfloor \{\psi\} .$$

The total mass is

$$M_T = m_o + \{\mu\}' [M] \{\mu\}$$

and the static mass moment about a pitch axis through point zero is

$$S = \{\mu\}' [M] \{\tau\} .$$

Therefore

$$M_T w_o + S \nu_o = -\omega^2 [A] \{\psi\} . \tag{36}$$

Multiplying Equation (32) by $\{\tau\}' [M]$ yields

$$\{\tau\}' [M] \{\psi\} - w_o \{\tau\}' [M] \{\mu\} - \nu_o \{\tau\}' [M] \{\tau\}$$

$$= \omega^2 \{\tau\}' [M] [C] [M] \{\psi\} .$$

Defining

$$[B] = \{\tau\}' [M] [C] [M]$$

and substituting from Equation (35)

$$-I_{m_o} \nu_o - w_o \{\tau\}' [M] \{\mu\} - \nu_o \{\tau\}' [M] \{\tau\} .$$

$$= \omega^2 [B] \{\psi\} .$$

The mass moment of inertia of total structure about a pitch axis through point zero is

$$I_{m_T} = I_{m_o} + \{\tau\} [M] \{T\} .$$

Therefore

$$I_{m_T} \nu_o + S w_o = - \omega^2 \lfloor B \rfloor \{\psi\}. \tag{37}$$

Solving Equation (37) for ν_o gives

$$\nu_o = - \frac{S w_o + \omega^2 \lfloor B \rfloor \{\psi\}}{I_{m_T}} . \tag{38}$$

Substituting this in Equation (36) and defining

$$W = I_{m_T} M_T - S^2$$

gives

$$w_o = \omega^2 \left[\frac{S}{W} \lfloor B \rfloor - \frac{I_{m_T}}{W} \lfloor A \rfloor \right] \{\psi\} . \tag{39}$$

Substituting this in Equation (38) gives

$$\nu_o = \omega^2 \left[\frac{S}{W} \lfloor A \rfloor - \frac{M_T}{W} \lfloor B \rfloor \right] \{\psi\} . \tag{40}$$

By satisfying the identities

$$[TT] \{\psi\} \equiv \lambda \{\mu\} w_o$$
$$[TR] \{\psi\} \equiv \lambda \{\tau\} \nu_o$$

it is seen that the T and R matrices are

$$\begin{aligned} [TT] &= \{\mu\} \left[\frac{S}{W} \lfloor B \rfloor - \frac{I_{m_T}}{W} \lfloor A \rfloor \right] \\ [TR] &= \{\tau\} \left[\frac{S}{W} \lfloor A \rfloor - \frac{M_T}{W} \lfloor B \rfloor \right] . \end{aligned} \tag{41}$$

4.1.2 FLEXIBILITY MATRIX. The inverted stiffness matrix is in reality the flexibility matrix of the system, i.e., it expresses displacements in terms of forces:

$$\{y\} = [C] \{P\} .$$

If the model is statically determinate, the development of the flexibility matrix directly is much simpler than inverting the stiffness matrix. However, if the structure is indeterminate, the calculation of the elements of the flexibility matrix becomes more complex, rapidly becoming involved and tedious with increasing numbers of redundancies. The element, C_{ij} of the flexibility matrix may be thought of as the deflection at point i resulting from a unit load at point j. The principle of reciprocal relations will force symmetry of the matrix, reducing the quantity of coefficients to be evaluated.

The flexibility matrix is formed by, first, developing individual flexibility matrices for each element in the system, considered as cantilevers.

$$\begin{Bmatrix} \bar{y}_l \\ \bar{\theta}_l \end{Bmatrix} = \begin{bmatrix} \delta\delta_l & \delta\theta_l \\ \theta\delta_l & \theta\theta_l \end{bmatrix} \begin{Bmatrix} P_l \\ M_l \end{Bmatrix} \tag{42}$$

Note that a) $\bar{y}_l$ and $\bar{\theta}_l$ are relative to the end considered fixed, and b) P_l and M_l are the total loads applied to the end considered free. Consequently, the total deflection value is found by transforming $\bar{y}_l$ and $\bar{\theta}_l$ from relative coordinates to absolute coordinates:

$$\begin{Bmatrix} y_i \\ \theta_i \end{Bmatrix} = \begin{bmatrix} T \end{bmatrix} \begin{Bmatrix} \bar{y}_i \\ \bar{\theta}_i \end{Bmatrix} . \tag{43}$$

The total applied loads, P_i and M_i, can be considered to be functions of the external loads applied to each mass of the structure, expressed by the transformation

$$\begin{Bmatrix} P_i \\ M_i \end{Bmatrix} = \begin{bmatrix} R \end{bmatrix} \begin{Bmatrix} p_i \\ m_i \end{Bmatrix} . \tag{44}$$

Thus the relationship between total deflection (y_i and θ_i) and the external loads applied to each mass (p_i and m_i) is developed by substituting the transformed values,

$$\begin{Bmatrix} \bar{y}_i \\ \bar{\theta}_i \end{Bmatrix} = \begin{bmatrix} C \end{bmatrix} \begin{Bmatrix} P_i \\ M_i \end{Bmatrix} ,$$

$$\begin{bmatrix} T \end{bmatrix} \begin{Bmatrix} \bar{y}_i \\ \bar{\theta}_i \end{Bmatrix} = \begin{bmatrix} T \end{bmatrix} \begin{bmatrix} C \end{bmatrix} \begin{bmatrix} R \end{bmatrix} \begin{Bmatrix} p_i \\ m_i \end{Bmatrix} ,$$

$$\begin{Bmatrix} y_i \\ \theta_i \end{Bmatrix} = \begin{bmatrix} T \end{bmatrix} \begin{bmatrix} C \end{bmatrix} \begin{bmatrix} R \end{bmatrix} \begin{Bmatrix} p_i \\ m_i \end{Bmatrix} ,$$

$$\begin{bmatrix} T \end{bmatrix} \begin{bmatrix} C \end{bmatrix} \begin{bmatrix} R \end{bmatrix} = \begin{bmatrix} C^* \end{bmatrix} = \text{coupled flexibility matrix} . \tag{45}$$

For a redundant structure, the influence coefficients are not so readily attained and use must be made of an appropriate static analysis such as virtual work on Castigliano's theorem (Reference 30).

An example of flexibility matrix for a determinant structure is given below:

Consider the three-mass cantilevered structure shown in Figure 11. The quantities p_i and m_i are the lateral force and moment applied to the structure at point i. If each element is considered to be a cantilever, fixed at the base, the free end deflection

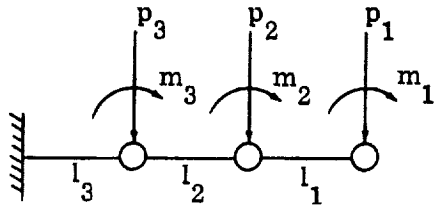

Figure 11. Three Mass Cantilevered Beam (Flexibility Matrix)

and rotation relative to the fixed base resultant from the total loads on the free end (external loads plus loads transmitted by the preceding element, if any), P_i and M_i, are found from the 2 x 2 flexibility matrix of the separated element:

$$\begin{Bmatrix} \bar{y} \\ \bar{\theta} \end{Bmatrix}_i = \begin{bmatrix} \delta\delta & \delta\theta \\ \theta\delta & \theta\theta \end{bmatrix}_i \begin{Bmatrix} P \\ M \end{Bmatrix}_i .$$

These relationships are independent of the rest of the structure, so the response for the entire system can be demonstrated by constructing a flexibility matrix composed of the 2 x 2 matrices of the individual elements:

$$\begin{Bmatrix} \bar{y}_1 \\ \bar{\theta}_1 \\ \bar{y}_2 \\ \bar{\theta}_2 \\ \bar{y}_3 \\ \bar{\theta}_3 \end{Bmatrix} = \begin{bmatrix} \delta\delta_1 & \delta\theta_1 & & & & \\ \theta\delta_1 & \theta\theta_1 & & & & \\ & & \delta\delta_2 & \delta\theta_2 & & \\ & & \theta\delta_2 & \theta\theta_2 & & \\ & & & & \delta\delta_3 & \delta\theta_3 \\ & & & & \theta\delta_3 & \theta\theta_3 \end{bmatrix} \begin{Bmatrix} P_1 \\ M_1 \\ P_2 \\ M_2 \\ P_3 \\ M_3 \end{Bmatrix} \quad (46) .$$

The total deflections of the three nodes of the structure, y_i and θ_i can be written in terms of the relative displacements, $\bar{y}_i$ and $\bar{\theta}_i$:

$$y_1 = \bar{y}_1 + \bar{y}_2 + \bar{y}_3 + l_1 \bar{\theta}_2 + \left(l_1 + l_2 \right) \bar{\theta}_3$$

$$\theta_1 = \bar{\theta}_1 + \bar{\theta}_2 + \bar{\theta}_3$$

$$y_2 = \bar{y}_2 + \bar{y}_3 + l_2 \bar{\theta}_3$$

$$\theta_2 = \bar{\theta}_2 + \bar{\theta}_3$$

$$y_3 = \bar{y}_3$$

$$\theta_3 = \bar{\theta}_3 \ .$$

In matrix form,

$$\begin{Bmatrix} y_1 \\ \theta_1 \\ y_2 \\ \theta_2 \\ y_3 \\ \theta_3 \end{Bmatrix} = \begin{bmatrix} 1 & 0 & 1 & l_1 & 1 & \left(l_1 + l_2 \right) \\ 0 & 1 & 0 & 1 & 0 & 1 \\ 0 & 0 & 1 & 0 & 1 & l_2 \\ 0 & 0 & 0 & 1 & 0 & 1 \\ 0 & 0 & 0 & 0 & 1 & 0 \\ 0 & 0 & 0 & 0 & 0 & 1 \end{bmatrix} \begin{Bmatrix} \bar{y}_1 \\ \bar{\theta}_1 \\ \bar{y}_2 \\ \bar{\theta}_2 \\ \bar{y}_3 \\ \bar{\theta}_3 \end{Bmatrix} . \qquad (47)$$

Combining Equation (46) and (47) yields,

$$\begin{Bmatrix} y_1 \\ \theta_1 \\ y_2 \\ \theta_2 \\ y_3 \\ \theta_3 \end{Bmatrix} = \begin{bmatrix} 1 & 0 & 1 & l_1 & 1 & (l_1 + l_2) \\ 0 & 1 & 0 & 1 & 0 & 1 \\ 0 & 0 & 1 & 0 & 1 & l_2 \\ 0 & 0 & 0 & 1 & 0 & 1 \\ 0 & 0 & 0 & 0 & 1 & 0 \\ 0 & 0 & 0 & 0 & 0 & 1 \end{bmatrix} \begin{bmatrix} \delta\delta_1 & \delta\theta_1 & & & & \\ \theta\delta_1 & \theta\theta_1 & & & & \\ & & \delta\delta_2 & \delta\theta_2 & & \\ & & \theta\delta_2 & \theta\theta_2 & & \\ & & & & \delta\delta_3 & \delta\theta_3 \\ & & & & \theta\delta_3 & \theta\theta_3 \end{bmatrix} \begin{Bmatrix} P_1 \\ M_1 \\ P_2 \\ M_2 \\ P_3 \\ M_3 \end{Bmatrix}$$

or

$$\begin{Bmatrix} y_1 \\ \theta_1 \\ y_2 \\ \theta_2 \\ y_3 \\ \theta_3 \end{Bmatrix} = \begin{bmatrix} \delta\delta_1 & \delta\theta_1 & \left(\delta\delta_2 + l_1\,\delta\theta_2\right) & \left(\delta\theta_2 + l_1\,\theta\theta_2\right) & \left(\delta\delta_3 + \left[l_1 + l_2\right]\theta\delta_3\right) & \left(\delta\theta_3 + \left[l_1 + l_2\right]\theta\theta_3\right) \\ \theta\delta_1 & \theta\theta_1 & \theta\delta_2 & \theta\theta_2 & \theta\delta_3 & \theta\theta_3 \\ 0 & 0 & \delta\delta_2 & \delta\theta_2 & \left(\delta\delta_3 + l_2\,\theta\delta_3\right) & \left(\delta\theta_3 + l_2\,\theta\theta_3\right) \\ 0 & 0 & \theta\delta_2 & \theta\theta_2 & \theta\delta_3 & \theta\theta_3 \\ 0 & 0 & 0 & 0 & \delta\delta_3 & \delta\theta_3 \\ 0 & 0 & 0 & 0 & \theta\delta_3 & \theta\theta_3 \end{bmatrix} \begin{Bmatrix} P_1 \\ M_1 \\ P_2 \\ M_2 \\ P_3 \\ M_3 \end{Bmatrix} \cdot \quad (48)$$

The total load at any element and can be related to the applied loads at each point by

$$P_1 = p_1 ,$$

$$M_1 = m_1 ,$$

$$P_2 = p_1 + p_2 ,$$

$$M_2 = m_1 + m_2 + l_2 p_1 ,$$

$$P_3 = p_1 + p_2 + p_3 ,$$

$$M_3 = m_1 + m_2 + m_3 + \left(l_1 + l_2\right) p_1 + l_2 p_2 ,$$

or, in matrix form

$$\begin{Bmatrix} P_1 \\ M_1 \\ P_2 \\ M_2 \\ P_3 \\ M_3 \end{Bmatrix} = \begin{bmatrix} 1 & 0 & 0 & 0 & 0 & 0 \\ 0 & 1 & 0 & 0 & 0 & 0 \\ 1 & 0 & 1 & 0 & 0 & 0 \\ l_1 & 1 & 0 & 1 & 0 & 0 \\ 1 & 0 & 1 & 0 & 1 & 0 \\ \left(l_1 + l_2\right) & 1 & l_2 & 1 & 0 & 1 \end{bmatrix} \begin{Bmatrix} p_1 \\ m_1 \\ p_2 \\ m_2 \\ p_3 \\ m_3 \end{Bmatrix} . \qquad (49)$$

Substituting this into equation (48) yields

$$\begin{Bmatrix} y_1 \\ \theta_1 \\ y_2 \\ \theta_2 \\ y_3 \\ \theta_3 \end{Bmatrix} = \begin{bmatrix} \delta\delta_1 & \delta\theta_1\left(\delta\delta_2 + l_1\,\delta\theta_2\right) & \left(\delta\theta_2 + l_1\,\theta\theta_2\right) & \left(\delta\delta_3 + \left[l_1 + l_2\right]\theta\delta_3\right) & \left(\delta\theta_3 + \left[l_1 + l_2\right]\theta\theta_3\right) \\ \theta\delta_1 & \theta\theta_1 & \theta\delta_2 & \theta\theta_2 & \theta\delta_3 & \theta\theta_3 \\ 0 & 0 & \delta\delta_2 & \delta\theta_2 & \left(\delta\delta_3 + l_2\,\theta\delta_3\right) & \left(\delta\theta_3 + l_2\,\theta\theta_3\right) \\ 0 & 0 & \theta\delta_2 & \theta\theta_2 & \theta\delta_3 & \theta\theta_3 \\ 0 & 0 & 0 & 0 & \delta\delta_3 & \delta\theta_3 \\ 0 & 0 & 0 & 0 & \theta\delta_3 & \theta\theta_3 \end{bmatrix} \begin{bmatrix} 1 & 0 & 0 & 0 & 0 & 0 \\ 0 & 1 & 0 & 0 & 0 & 0 \\ 1 & 0 & 1 & 0 & 0 & 0 \\ l_1 & 1 & 0 & 1 & 0 & 0 \\ 1 & 0 & 1 & 0 & 1 & 0 \\ \left(l_1 + l_2\right) & 1 & l_2 & 1 & 0 & 1 \end{bmatrix} \begin{Bmatrix} p_1 \\ m_1 \\ p_2 \\ m_2 \\ p_3 \\ m_3 \end{Bmatrix}$$

which is equal to

$$
\begin{Bmatrix} y_1 \\ \theta_1 \\ y_2 \\ \theta_2 \\ y_3 \\ \theta_3 \end{Bmatrix} =
\begin{bmatrix}
\left(\delta\delta_1+\delta\delta_2+\delta\delta_3+l_1\left[\delta\theta_2+\theta\delta_2\right]+\left[l_1+l_2\right]\left[\delta\theta_3+\theta\delta_3\right]+l_1^2\theta_1\theta_2+\left[l_1+l_2\right]^2\theta\theta_3\right) & \left(\delta\theta_1+\delta\theta_2+\delta\theta_3+l_1\theta_1\theta_2+\left[l_1+l_2\right]\theta\theta_3\right) & \left(\delta\delta_2+\delta\delta_3+l_1\delta\theta_2+l_2\delta\theta_3+\left[l_1+l_2\right]\theta\delta_3+l_2\left[l_1+l_2\right]\theta\theta_3\right) & \left(\delta\theta_2+\delta\theta_3+l_1\theta\theta_2+\left[l_1+l_2\right]\theta\theta_3\right) & \left(\delta\delta_3+\left[l_1+l_2\right]\theta\delta_3\right) & \left(\delta\theta_3+\left[l_1+l_2\right]\theta\theta_3\right) \\
\left(\theta\delta_1+\theta\delta_2+\theta\delta_3+l_1\theta\theta_2+\left[l_1+l_2\right]\theta\theta_3\right) & \left(\theta\theta_1+\theta\theta_2+\theta\theta_3\right) & \left(\theta\delta_2+\theta\delta_3+l_2\theta\theta_3\right) & \left(\theta\theta_2+\theta\theta_3\right) & \theta\delta_3 & \theta\theta_3 \\
\left(\delta\delta_2+\delta\delta_3+l_1\delta\theta_2+l_2\theta\delta_3+\left[l_1+l_2\right]\delta\theta_3+l_2\left[l_1+l_2\right]\theta\theta_3\right) & \left(\delta\theta_2+\delta\theta_3+l_2\theta\theta_3\right) & \left(\delta\delta_2+\delta\delta_3+l_2\left[\theta\delta_3+\delta\theta_3\right]+l_2^2\theta\theta_3\right) & \left(\delta\theta_2+\delta\theta_3+l_2\theta\theta_3\right) & \left(\delta\delta_3+l_2\theta\delta_3\right) & \left(\delta\theta_3+l_2\theta\theta_3\right) \\
\left(\theta\delta_2+\theta\delta_3+l_1\theta\theta_2+\left[l_1+l_2\right]\theta\theta_3\right) & \left(\theta\theta_2+\theta\theta_3\right) & \left(\theta\delta_2+\theta\delta_3+l_2\theta\theta_3\right) & \left(\theta\theta_2+\theta\theta_3\right) & \theta\delta_3 & \theta\theta_3 \\
\left(\delta\delta_3+\left[l_1+l_2\right]\delta\theta_3\right) & \delta\theta_3 & \left(\delta\delta_3+l_2\delta\theta_3\right) & \delta\theta_3 & \delta\delta_3 & \delta\theta_3 \\
\left(\theta\delta_3+\left[l_1+l_2\right]\theta\theta_3\right) & \theta\theta_3 & \left(\theta\delta_3+l_2\theta\theta_3\right) & \theta\theta_3 & \theta\delta_3 & \theta\theta_3
\end{bmatrix}
\begin{Bmatrix} p_1 \\ m_1 \\ p_2 \\ m_2 \\ p_3 \\ m_3 \end{Bmatrix}
$$

Noting that $\theta\delta_i = \delta\theta_i$ for a cantilevered beam, the above flexibility matrix is symmetric and defines the deflection at any point i in terms of loads at points j.

Equation 50

4.1.3 TRANSFORMED MASS MATRIX. Another alternative technique for forming the dynamic matrix is to transform the coordinate system from the absolute to the relative sense. The equations of motion formed previously consider the displacements of the respective coordinates to be referenced to a fixed point, or neutral position. The displacements may also be expressed relatively - referenced to an adjacent coordinate. Furthermore, the inherent relationship between the displacements in absolute terms, y, and the displacements in relative terms, $\bar{y}$, is readily expressed by a simple transformation matrix:

$$\{y\} = [T] \{\bar{y}\} .$$

For example, the simple cantilevered beam in Figure 12 has six coordinates. The relative-absolute relationship is given by:

$$y_1 = \bar{y}_1 + \bar{y}_2 + \bar{y}_3 + l_1 \bar{\theta}_2 + (l_1 + l_2) \bar{\theta}_3 ,$$

$$y_2 = \bar{y}_2 + \bar{y}_3 + l_2 \bar{\theta}_3 ,$$

$$y_3 = \bar{y}_3 ,$$

$$\theta_1 = \bar{\theta}_1 + \bar{\theta}_2 + \bar{\theta}_3 ,$$

$$\theta_2 = \bar{\theta}_2 + \bar{\theta}_3 ,$$

$$\theta_3 = \bar{\theta}_3 .$$

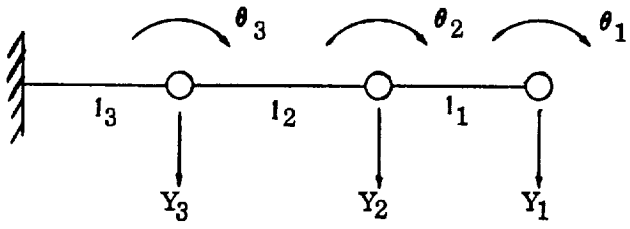

Figure 12. Three Mass Cantilevered Beam

Thus,

$$\begin{Bmatrix} y_1 \\ y_2 \\ y_3 \\ \theta_1 \\ \theta_2 \\ \theta_3 \end{Bmatrix} = \begin{bmatrix} 1 & 1 & 1 & 0 & l_2 & (l_2+l_3) \\ 0 & 1 & 1 & 0 & 0 & l_3 \\ 0 & 0 & 1 & 0 & 0 & 0 \\ 0 & 0 & 0 & 1 & 1 & 1 \\ 0 & 0 & 0 & 0 & 1 & 1 \\ 0 & 0 & 0 & 0 & 0 & 1 \end{bmatrix} \begin{Bmatrix} \bar{y}_1 \\ \bar{y}_2 \\ \bar{y}_3 \\ \bar{\theta}_1 \\ \bar{\theta}_2 \\ \bar{\theta}_3 \end{Bmatrix} \tag{51}$$

or

$$\{y\} = [T]\{\bar{y}\}.$$

The kinetic and potential energies of the system can then be written (in matrix notation) in terms of relative coordinates as,

$$2KE = \{\dot{\bar{y}}\}' [T]' [M] [T] \{\dot{\bar{y}}\}$$

$$2PE = \{\bar{y}\}' [C^{-1}] \{\bar{y}\}.$$

where C is the uncoupled flexibility matrix consisting of 2 x 2 matrices for cantilevered elements. Using La Grange's equation

$$\frac{d}{dt}\left(\frac{\partial KE}{\partial \dot{y}_i}\right) + \frac{\partial PE}{\partial y_i} + \frac{\partial W}{\partial y_i} = 0 \qquad (52)$$

the equations of motion become

$$\left[T\right]' \left[M\right]\left[T\right]\left\{\ddot{\bar{y}}\right\} + \left[C^{-1}\right]\left\{\bar{y}\right\} = 0 \qquad (53)$$

and the dynamic matrix is

$$\left[\left[C\right]\left[T\right]'\left[M\right]\left[T\right]\right]\left\{\psi\right\} = \lambda\left\{\psi\right\} \qquad (54)$$

This approach is very similar to the method in the previous section with the transformation of coordinates coupling the mass matrix instead of the flexibility matrix. Note that the modes, $\{\psi\}$, are in terms of relative coordinates and must be premultiplied by the transform matrix, $[T]$, to obtain absolute vectors.

4.2 SOLUTIONS FOR CHARACTERISTICS

Formulation of the equations of motion of dynamic systems results in a linear differential equation for the continuous exact solution or a series of differential equations for the approximate solutions. For lateral vibration usually only the lower modes are of any significance and therefore the approximate solutions are of practical importance. Two methods are used to describe the system in these approximate solutions: (1) the system is divided into a finite number of segments connected by massless stiffness and (2) the system is described in terms of assumed functions. Solving for the characteristics of the resulting equations can be categorized into three groups. These are: (1) energy methods, (2) solving the differential equation, and (3) solving the integral equation. The equations are in the general matrix form:

$$-\omega^2\left[M\right]\left\{z\right\} + \left[K\right]\left\{z\right\} = 0 \quad \text{(differential equation)} \qquad (55)$$

or

$$\left\{z\right\} = \omega^2\left[K\right]^{-1}\left[M\right]\left\{z\right\} \quad \text{(integral equation)} \qquad (56)$$

The most general solution of Equation (55) involves expansion of the determinant and solving the polynomial equation. This procedure is adequate for simple systems and up to four degrees of freedom can be solved easily. Methods for higher order systems have been developed in References 31 and 32. However, since only the lower modes are important some approximate methods have been developed which obtain these modes and frequencies with sufficient accuracy.

4.2.1 MATRIX ITERATION (STODOLA AND VIANELLO METHOD). The matrix iteration technique is essentially the Stodola and Vinanello method in matrix form. The integral equation is

$$\{z\} = \omega^2 [K]^{-1} [M] \{z\} \cdot \tag{57}$$

It can be seen that $\omega^2 [M] \{Z_{n-1}\}$, is the load associated with a assumed mode shape, $\{Z_{n-1}\}$, vibrating at a frequency ω. The deflection resulting from this load or the next approximation of the mode shape is obtained by premultiplication by the influence coefficients, or the inverse of the stiffness matrix. Since ω^2 is a constant it can be assumed to be unity and the equation becomes

$$\{Z_n\} = [K]^{-1} [M] \{Z^*_{n-1}\} \cdot \tag{58}$$

where $\{Z^*\}$ is a vector normalized on its largest element. Successive iterations of Equation (58) continue until $\{Z_n^*\}$ has converged, i.e., every element in $\{Z_n^*\}$ satisfies

$$\{Z_n^*\} - \{Z^*_{n-1}\} \leq \delta \cdot$$

The frequency of the mode is then

$$\omega^2 = \frac{1}{Z_{n1}} \tag{59}$$

where Z_{n1} is the largest element of the unnormalized vector $\{Z_n\}$. Proof of convergence is given in Reference 33.

For most practical problems it is necessary to obtain more than the first normal mode. This is accomplished by applying the condition of orthogonality as a means of purifying the assumed higher modes of lower mode components. The orthogonality condition requires that

$$\{\psi_1\}' [M] \{\psi_2\} = 0 . \tag{60}$$

Therefore, modification of the dynamic matrix to satisfy this condition will allow extraction of the next mode. This is expressed in matrix form as:

$$[D_2] = [D_1] [[I] - [\Lambda]] \tag{61}$$

where $[I]$ is a unity matrix and $[\Lambda]$ is a matrix of zero's except for the row (or rows) imposing the orthogonality. This row is composed of the elements $Z_i m_i$ normalized on its largest element. This element locates the characteristic row and the row matrix is a good approximation of the characteristic row. As an example,

$$[Z_j' m] = [Z_{11} m_1 \quad Z_{21} m_2 \quad Z_{31} m_3 \quad Z_{41} m_4] .$$

If $Z_{31} m_3$ is the largest element, then

$$[\Lambda] = \begin{bmatrix} 0 & 0 & 0 & 0 \\ 0 & 0 & 0 & 0 \\ \frac{Z_{11} m_1}{Z_{31} m_3} & \frac{Z_{21} m_2}{Z_{31} m_3} & 1 & \frac{Z_{41} m_4}{Z_{31} m_3} \\ 0 & 0 & 0 & 0 \end{bmatrix} .$$

Once $[\Lambda]$ is obtained then D_2 can be formed and iterations proceed to determine the next mode and frequency.

For improved accuracy and subsequent deflation of the D matrix it is recommended that iterations be performed on the row matrix, $\lfloor X_j' M \rfloor$, by post multiplication by the dynamic matrix. This removes errors in roundoff in the preceeding fundamental mode and provides a more accurate characteristic. Thus,

$$\overline{\lfloor Z_j' \quad M \rfloor} [D] = \lfloor Z_j' \quad M \rfloor$$

where $[\ \overline{\ }\ ]$ indicates normalization on its largest element. $\lfloor Z_j' M \rfloor$ is then normalized on its largest element and placed in the $[\Lambda]$ matrix. If the characteristic row is found by this method, the deflated dynamic matrix for successive modes can then be obtained by

$$[D_3] = [D_2] \left[[I] - [\Lambda_2]\right].$$

If the deflated matrix is obtained only from the conditions of orthogonality, then

$$[D_n] = [D_1] \left[[I] - [\Lambda_n]\right]. \tag{62}$$

where $[\Lambda_n]$ satisfies orthogonality between first and n, second and n, ---, and n-1 and n modes.

An alternate method for deflating the matrix is given in Reference 34 and is particularly useful in application with automatic computers. This deflation method gives

$$[D_2] = [D_1] - \frac{1}{\omega_1^2} \{Z_1\} \lfloor Z_1 \rfloor [M] \tag{63}$$

where $\{Z_1\}$ is the column of elements of the first mode normalized so that $\lfloor Z_1 \rfloor [M] \{Z_1\} = 1$. For each succeeding mode the matrix is modified by subtracting the triple matrix product for the proceeding mode from the proceeding modified dynamic matrix

$$[D_n] = [D_{n-1}] - \frac{1}{\omega^2_{n-1}} \{Z_{n-1}\} \lfloor Z_{n-1} \rfloor [M] . \tag{64}$$

4.2.2 HOLZER-MYKLESTAD METHOD. The Holzer-Myklestad method is extremely suitable for obtaining solution of the differential equations of beams represented as concentrated masses connected by massless stiffness elements. A principle advantage of this method is that each mode is obtained independently and therefore all modes are as accurate as represented by the system analyzed.

The technique proposed by Holzer was originally developed for torsional systems. It is equally applicable to any close-coupled system, i.e. represented as a spring mass system. A frequency is assumed and one element of the mode shape vector is taken as unity. Through equilibrium equations, the other elements of the vector are calculated. There will be one additional equilibrium equation left after the last element of the mode shape vector is evaluated, which will be satisfied only if the assumed frequency is correct. Successive frequency trials are made until the proper value is obtained. The process is facilitated by plotting net unbalanced force on the final mass against frequency. At the natural frequencies of the system, the curve of net force passes through zero.

As an example, consider the simple system of two masses and two springs shown in Figure 13. The governing equations are

$$\begin{aligned} m_1 \ddot{X}_1 + K_1 X_1 - K_1 X_2 &= 0 \\ m_2 \ddot{X}_2 - K_1 X + (K_1 + K_2) X_2 &= 0 . \end{aligned} \tag{65}$$

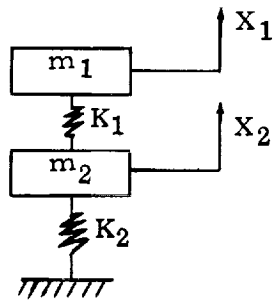

Figure 13. Two Degree of Freedom Spring-Mass System

The assumption of harmonic motion reduces these equations to

$$\left(-\omega^2 m_1 + K_1\right)X_1 - K_1 X_2 = 0$$

$$-K_1 X_1 + \left(-\omega^2 m_2 + K_1 + K_2\right)X_2 = 0$$

Let $\omega_1^2 = \omega^2$ and $X_1 = 1$. From the first equation:

$$X_2 = \frac{K_1 - \omega^2 m_1}{K_1} \tag{66}$$

and from the second equation,

$$-K_1 + \left(K_1 - \omega^2 m_2 + K_2\right)\left(\frac{K_1 - \omega^2 m_1}{K_1}\right) = 0 . \tag{67}$$

The magnitude of the left hand side of this equation can be plotted against frequency. It may be facilitated by calculations made in tabular form:

ω^2	K_1	$-\omega^2 m_1$	$-\omega^2 m_2$	$\frac{K_1 - \omega^2 m_1}{K_1} = X_2$	$K_1 - \omega^2 m_2 + K_2$	Residual
0	K_1	0	0	1	$K_1 + K_2$	K_2

When the residual is zero, the correct frequency has been obtained.

Branched systems will necessitate temporarily expressing some elements of the mode shape vector in terms of others, but in all systems, numerical values for the entire mode shape will be determined upon solution of the next to last equilibrium equation, leaving the last equation for frequency evaluation.

As an example consider the simple three mass system shown in Figure 14.

$$m_1 \ddot{X}_1 + (K_1 + K_3) X_1 - K_1 X_2 - K_3 X_3 = 0$$

$$m_2 \ddot{X}_2 - K_1 X_1 + (K_1 + K_2 + K_4) X_2 - K_4 X_3 = 0$$

$$m_3 \ddot{X}_3 - K_3 X_1 - K_4 X_2 + (K_1 + K_4) X_3 = 0$$

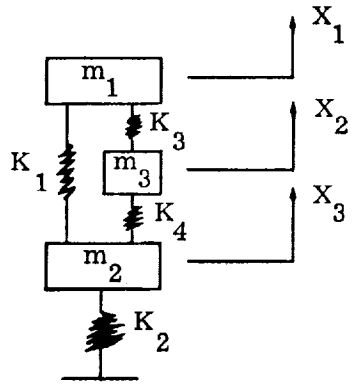

Figure 14. Three Degree of Freedom Spring-mass System

Introducing harmonic motion results in

$$(K_1 + K_3 - \omega^2 m_1) X_1 - K_1 X_2 - K_3 X_3$$

$$- K_1 X_1 + (K_1 + K_2 + K_4 - \omega^2 m_2) X_2 - K_4 X_3 = 0$$

$$- K_3 X_1 - K_4 X_2 + (K_1 + K_4 - \omega^2 m_3) X_3 = 0$$

Let $X_1 = 1$, and from the first equation

$$X_3 = \frac{K_1 + K_3 - \omega^2 m_1 - K_1 X_2}{K_3} .$$

From the third equation

$$- K_3 - K_4 X_2 + \left(K_1 + K_4 - \omega^2 m_3\right) \left(\frac{K_1 + K_3 - \omega^2 m_1 - K_1 X_2}{K_3} \right) = 0$$

or

$$- K_3 + \left(K_1 + K_4 - \omega^2 m_3\right) \left(\frac{K_1 + K_3 - \omega^2 m_1}{K_3} \right) - \left[K_4 + \frac{K_1}{K_3} \left(K_1 + K_4 - \omega^2 m_3 \right) \right] X_2 = 0$$

$$X_2 = \frac{\left(K_1 + K_4 - \omega^2 m_3\right)\left(K_1 + K_3 - \omega^2 m_1\right) - K_3^2}{K_3 K_4 + K_1 \left(K_1 + K_4 - \omega^2 m_3\right)} = A . \quad (68)$$

Hence

$$X_3 = \frac{K_1 + K_3 - \omega^2 m_1 - K_1 A}{K_3} = B . \quad (69)$$

And finally, from the second equation

$$- K_1 + \left(K_1 + K_2 + K_4 - \omega^2 m_2\right) A - K_3 B = 0 . \quad (70)$$

The three frequencies which satisfy this equation are the natural frequencies and are determined by tabular methods as in the previous example.

In reality, the Myklestad method is the Holzer method extended to include far-coupled systems, i.e. beam systems. The slope and deflection at one end of a beam segment are expressible in terms of the slope and deflection at the other end, the loads at the other end and the flexibility of the beam segment. The boundary conditions at one end of the beam give an initial set of values. Two of the four conditions will be unknown. One is set to unity and the interior values are determined in terms of the remaining unknown.

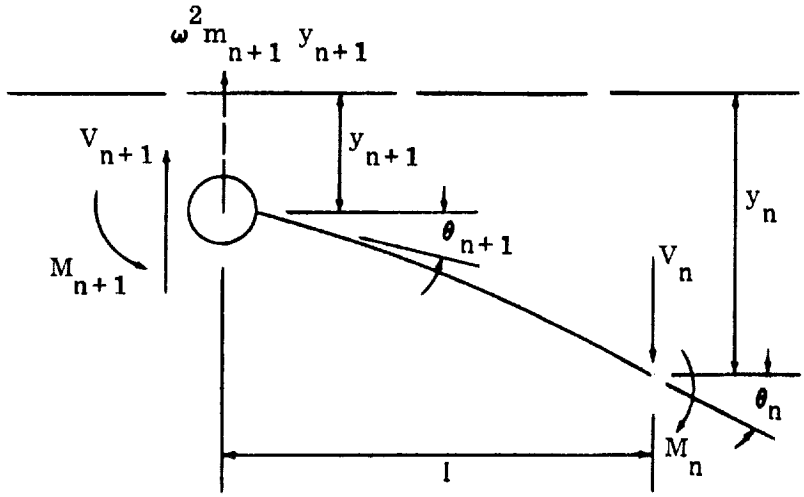

Figure 15. Free-Body Diagram of Vibrating Beam Segment

As an illustration, consider the beam segment in Figure 15. The deflections and forces at the left end can be expressed as:

$$\left.\begin{aligned} V_{n+1} &= V_n - m_{n+1}\ \omega^2\ y_{n+1} \\ M_{n+1} &= M_n + V_n\ l \\ y_{n+1} &= y_n - V_n\ (\delta\delta) - M_n\ (\delta\theta) - l\theta_n \\ \theta_{n+1} &= \theta_n - V_n\ (\theta\delta) - M_n\ (\theta\theta) \end{aligned}\right\} \qquad (71)$$

The quantities $(\delta\delta), (\delta\theta), (\theta\delta), (\theta\theta)$ are the flexibility influence coefficients of the beam. If the right end of the beam segment is the end of the total beam (let n = 1), two of the four valables at that end can be determined from the end conditions: for a free end. M_1 is zero and V_1 is equal to the inertia force $m_1 \omega^2 y_1$. Of the two remaining conditions, one is assigned a value of unity and analysis is carried out in terms of the other. For the free end, X_1 is assigned a unity value (making $V_1 = m_1 \omega^2$). The four variables at point two may be evaluated as:

$$y_2 = 1 - m_1 \omega^2(\delta\delta) - l_1 \theta_1 ,$$

$$\theta_2 = \theta_1 - m_1 \omega^2 (\theta\delta) ,$$

$$M_2 = m_1 \omega^2 l ,$$

$$V_2 = m_1 \omega^2 - m_2 \omega^2 \left[1 - m_1 \omega^2(\delta\delta) - l_1\theta_1 \right] .$$

If an arbitrary value for ω^2 is assigned, each of the four variables at point two reduces to an expression involving a constant and a coefficient times θ_1.

The variables at the next point on the beam may be expressed in terms of those just obtained by using Equation (71) and will also be in linear terms of θ_1. The evaluations may thus be propagated across the beam, with the ultimate result that the four variables at the far end of the beam are expressed as linear functions of θ_1.

From the end conditions at this point, the values of two of these variables will be known. One of these known quantities is used to evaluate θ_1, which is then substituted into the expression for the second known variable. For the correct value of ω^2, the expression will produce the known value; otherwise, an error term or residual will be obtained. Several trial values of ω^2 are made, repeating the propagation process each time. If the resultant residuals are plotted against ω^2, the extraction of the proper values of ω^2 is facilitated by extrapolation of the curve. The natural frequencies occur where the curve crosses the axis. Higher frequencies are obtained independently, thus are independent of any inaccuracies which may exist in calculated lower modes.

4.2.3 ENERGY METHODS. Lord Rayleigh's method of evaluating the fundamental frequency of a system is based on the principle of conservation of energy. At the maximum deformation of the system vibration in its fundamental frequency, all the energy of the system is in a potential energy from $\left(PE = \frac{1}{2} \int EI \left(\frac{d^2y}{dx^2} \right)^2 dx \right)$. But at the instant the system passed through the equilibrium position, its energy is entirely in kinetic form $\left(KE = \frac{1}{2} \int m\dot{y}^2 \, dx \right)$. If energy is conserved, the maximums of those two values may be equated. A deflection shape is assumed and for harmonic motion, $y = U \sin \omega t$, and hence,

$$\dot{y} = \omega U \cos \omega t$$

$$\frac{1}{2} \int EI \left(\frac{d^2U}{dx^2} \right)^2 dx = \frac{1}{2} \int m U^2 \omega^2 \, dx , \qquad (72)$$

and thus

$$\omega^2 = \frac{\int EI \left(\frac{d^2U}{dx^2} \right)^2 dx}{\int m U^2 \, dx} . \qquad (73)$$

It can be shown that close approximations to the fundamental frequency are obtained even if the assumed deflection shape is not very close to the true shape.

The Rayleigh method was generalized by Ritz to give more accurate values for the frequencies as well as to give estimates for several mode frequencies at one time. Basically, Ritz suggested that the assumed deflection curve be expressed as the sum of several functions in the form

$$y = \Sigma f_n (x) q_n . \tag{74}$$

The more functions and constants introduced the more accurate will be the value of the fundamental frequency. Also if n functions are introduced estimates on the first n mode frequencies will be obtained. Having expressed the assumed deflection curve in terms of n functions f (x), the kinetic and potential energies (omitting shear & rotary inertias) are expressed as

$$2\,KE = \int m (x) \dot{y} (x, t) dx \tag{75}$$

$$2\,PE = \int EI (x) \left(\frac{d^2 y}{dx^2}\right)^2 dx . \tag{76}$$

Substituting Equation (74) into Equations (75) and (75),

$$2\,KE = \sum_{i=1}^{n} \sum_{j=1}^{n} m_{ij} q_i q_j \tag{77}$$

$$2\,PE = \sum_{i=1}^{n} \sum_{j=1}^{n} K_{ij} q_i q_j \tag{78}$$

where $$K_{ij} = \int EI \frac{d^2}{dx^2} \left[f_i (x) \right] \frac{d^2}{dx^2} \left[f_j (x) \right] dx$$

and $$m_{ij} = \int m \frac{d^2}{dx^2} \left[f_i (x) \right] \frac{d^2}{dx^2} \left[f_j (x) \right] dx .$$

Substituting Equation (77) and (78) into La Grange's Equation gives the differential equations

$$\sum_{j=1}^{n} m_{ij} \ddot{q}_j + \sum_{j=1}^{n} K_{ij} q_j = 0 . \qquad (79)$$

Putting as a solution $q_j = \bar{q} \sin \omega t$

$$\sum_{j=1}^{n} (K_{ij} - \omega^2 m_{ij}) \bar{q}_j = 0 \qquad (80)$$

or a set of algebraic equations equal in number to the number of unknown coefficients. The determinantal equation for the set will yield frequencies for the first n modes of vibration and eigenvectors which when multiplied by the assumed functions give approximate mode shapes.

The result gives good accuracy in frequency but poor agreement with mode shape. Using the mode shape obtained as a second approximation improves frequency accuracy and greatly improves mode shape.

Also, expressing the strain energy in terms of inertial loading rather than the assumed deflections increases the flexibility of this method in that shear deformation and rotary inertias are then easily included.

4.2.4 MODAL QUANTITIES. Solutions to the characteristic equations give the reciprocals of the squares of the circular frequencies and also the mode shapes of the restrained system. The linear frequencies of vibration are obtained from the circular frequencies. If each mode shape, $\{\psi\}_n$ is considered to be the nth column of a matrix $[\Phi]$ of all the mode shapes then, $[\Phi]' [M] [\Phi]$ is an orthogonality check of the mode shapes. The diagonal element $([\Phi]' [M][\Phi])$ is called the generalized mass of the system for the mode n. (The generalized mass of the system may be considered to be a measure of the kinetic energy of the system). In this discussion the vector $\{\psi\}$ was stated to be mode shape of the structural system. For a restrained system, $\{\psi\}$ is the complete mode shape. For a free-free system the displacements due to w_o and ν_o must be added to obtain the complete mode shape. Also, for a free-free system, the generalized mass must be modified to include the contribution of the temporarily fixed point.

The slope of a node of a beam as computed by the foregoing is not the total slope of the beam at the node. The slope computed is the slope due to beam bending. To obtain the total slope, the shearing slope of the beam must be added to the slope due to beam bending. This is done by

$$\{\beta\} = \{\theta\} + \{\gamma\} \tag{81}$$

where $\{\gamma\} = [SS]\{FB\}$

and,

$\{\beta\}$ = total slopes of a beam element,

$\{\theta\}$ = bending slopes of a beam element,

$\{\gamma\}$ = shearing slopes of a beam element,

$\{FB\}$ = internal forces on a beam element, and

$\{SS\}$ = shear - slope matrix .

The matrix $[SS]$ is a diagonal matrix whose elements are 1/KAG at the nodes of a beam element.

The generalized forces of the restrained system may be obtained from either Equation (31) or Equation (27) depending upon whether or not there are any zero generalized force boundary conditions. Rather than use Equation (31), another equivalent relationship is used. Extending Equation (31)

$$\{F_f\} = [K][\psi] = \omega^2[M]\{\psi\} . \tag{82}$$

Equation (82) is used instead of Equation (31) when calculating the generalized forces of the restrained system. Using Equation (30) the generalized displacements that have zero generalized forces are calculated. For a free-free system Equation (30) is modified slightly. In its stated form Equation (30) would compute generalized displacements with respect to the temporarily fixed point. For a free-free system the analogy to Equation (30) is :

$$\left\{ \rho_f \right\} = \left[g \right]^{-1} \left[e \right]' \left\{ \mu \, w_o + \tau \, \nu_o - \psi_f \right\} + \left\{ \mu' \right\} w_o + \left\{ \tau \right\} \nu_o \qquad (83)$$

where μ, τ, w_o and ν_o have previously been defined, and μ' and τ' have the same meaning as μ and τ. However, μ and τ refer to the mode shape, $\{\psi\}$, and μ' and τ' refer to the generalized displacements that have zero generalized forces, $\{\rho_f\}$. The generalized forces that have zero generalized displacements are obtained from Equation (28). The internal forces and/or moments (shears and/or bending moments) of each element are obtained from:

$$\left\{ P \right\} = \left[K \right] \left\{ y \right\} .$$

4.3 MODE SYNTHESIS ANALYSIS

The complicating aspects of the clustered booster vehicle have, as a net effect, the requirement of large numbers of coordinates in the model. The resultant size of the governing equations may well be so large as to overwhelm the best of analysts or computers. The technique of modal synthesis is a process whereby the dynamic characteristics of the several components of the system are calculated separately, and then brought together to evaluate the dynamic characteristics of the entire system. This technique is also applicable to the analysis of staged vehicles in that the natural vibration characteristics of the individual stages can be computed separately and combined via modal synthesis to determine the characteristics of the entire vehicle.

The entire concept of modal synthesis is founded on the principal that a component is completely (or adequately) represented by its primary modes and if this is true, then the connections of these components at their interfaces can be described in terms of the component modal quantities. A set of equations can be written with coordinates in terms of component mode shapes and amplitude factors. Solving these equations for the amplitude factors and multiplying by the component modes will give system modes.

The division of the system into components can be done by removal of connecting flexibility elements. The parts thus formed will constitute free system i.e., not attached to a fixed point. It is assumed that the components will be defined in such a way that determination of their individual dynamic characteristics does not become a complicated task and consequently, the techniques previously discussed regarding the analysis of simple systems may be utilized to provide these dynamic characteristics.

For the free components, complete description of motion requires the rigid body translation and rotation modes and the elastic modes. Thus, if the component is in beam form, the lateral deflection of point is given by:

$$y_i = Y + L_i \Theta + \Sigma_n \phi_{in} \eta_n$$

where

y_i is the lateral displacement of point i ,

Y is the rigid body lateral translation of the component c. g. ,

L_i is the distance between the component c. g. and point i ,

Θ is the rigid body rotation of the component c. g. ,

η_n is the appropriate weighting factor applied to mode n , and

ϕ_{in} is the lateral displacement of point i in mode n .

The rotation of point i is given by

$$\theta_i = \Theta + \Sigma_n \alpha_{in} \eta_n$$

where

θ_i is the angular displacement of point i , and

α_{in} is the slope at point i in node n .

A simple component beam will have its coordinate motions expressed in matrix form as:

$$\begin{Bmatrix} y_1 \\ \vdots \\ y_k \\ \theta_1 \\ \vdots \\ \theta_k \end{Bmatrix} = \begin{bmatrix} 1 & L_1 & \phi_{11} \cdots \phi_{1m} \\ \vdots & \vdots & \vdots \\ 1 & L_k & \phi_{k1} \cdots \phi_{km} \\ 0 & 1 & \alpha_{11} \cdots \alpha_{1m} \\ \vdots & \vdots & \vdots \\ 0 & 1 & \alpha_{k1} \cdots \alpha_{km} \end{bmatrix} \begin{Bmatrix} Y \\ \Theta \\ \eta_1 \\ \vdots \\ \eta_m \end{Bmatrix} . \qquad (84)$$

More generally

$$\{y\} = \left[TS\right] \left\{ \begin{matrix} Y \\ \eta \end{matrix} \right\}.$$

For a system composed of several component beams

$$\left\{ \begin{matrix} y^{(1)} \\ y^{(2)} \\ \vdots \\ y^{(S)} \end{matrix} \right\} = \left[\begin{matrix} TS^{(1)} & & \\ & TS^{(2)} & \\ & & \ddots \\ & & & TS^{(S)} \end{matrix} \right] \left\{ \begin{matrix} \eta^{(1)} \\ \eta^{(2)} \\ \vdots \\ \eta^{(S)} \end{matrix} \right\}. \qquad (85)$$

The kinetic energy of the system is then

$$2KE = \dot{\eta}' (TS)' M (TS) \dot{\eta}.$$

and

$$\frac{d}{dt} \left(\frac{\delta KE}{\delta \dot{\eta}} \right) = (TS)' M (TS) \ddot{\eta}$$

where M is a diagonal of system masses.

Note that $(TS)' M (TS)$ is a diagonal of the generalized masses of modes used in the representation

$$(TS)' M (TS) \ddot{\eta} = \left[\begin{matrix} m^{(1)} & & \\ & m^{(2)} & \\ & & \ddots \\ & & & m^{(S)} \end{matrix} \right] \left\{ \begin{matrix} \ddot{\eta}^{(1)} \\ \ddot{\eta}^{(2)} \\ \vdots \\ \ddot{\eta}^{(S)} \end{matrix} \right\}. \qquad (86)$$

Similarly, the potential energy in the component modes can be expressed as

$$2\,PE = \eta'(TS)'\,K\,(TS)\,\eta$$

and the energy in the connecting elements can be expressed as $\Sigma_k \; K_{ck}\Delta_k$ where K_{ck} is the stiffness of the connecting element and, Δ_k is the deformation of that element. If y_r and θ_r describe the coordinate displacements of the components, then

$$\{\Delta\} = [RC]\begin{Bmatrix} y_r \\ \theta_r \end{Bmatrix} = (RC)\;(TS)\;\eta \tag{87}$$

where (RC) is a transformation matrix expressing the relation between Δ_k and the component displacements. The potential energy is given by

$$2\,PE = \eta'\,(TS)'\,(RC)'\,K_c\,(RC)\;(TS)\;\eta$$

and the total potential energy of the system

$$2\,PE = \eta'\,(TS)'\,(RC)'\,K_c\,(RC)'\,(TS)\;\eta + \eta\;\;(TS)'\,K\;(TS)\;\eta$$

$$\frac{\partial PE}{\partial \eta} = \left[(TS)'\,(RC)'\,K_c\;(RC)\;(TS) \;\;+\;\; (TS)'\,K\;(TS)'\right]\eta\,.$$

It is shown in Reference 35 that

$$(TS)'\,K\;(TS) = \left[\omega^2 m\right].$$

Therefore, the complete set of equations is

$$\left[m\right]\{\ddot{\eta}\} + \left[\left[\omega^2 m\right] + \left[(TS)'\,(RC)'\,K_c\,(RC)\;(TS)\right]\right]\;\{\eta\} = 0 \tag{88}$$

There are other ways to develop a modal synthesis technique for complex systems which are quite valid. But the approach presented above enables the analyst to evaluate a minimum of physical parameters, then manipulate them with matrix techniques, which are readily adaptable to computer programming, into the final form of the governing equation: the parameters to be obtained are just the component modal properties (mode shapes, generalized masses, frequencies), the coordinate displacements in terms of the rigid body displacements and modal weighting factors (the [TS] transformation matrix), and the deformations of the connecting elements in terms of the coordinate displacements (the [RC] transformation matrix). The final governing equation may be formed immediately from these data. Solutions for these equations can be obtained by the methods given in Section 4.2.

These roots will be the frequencies of the coupled system, and the vectors $\{\eta\}$, when premultiplied by [TS] will give the system modes.

To demonstrate the modal synthesis technique, consider the spring-mass system of Figure 16.

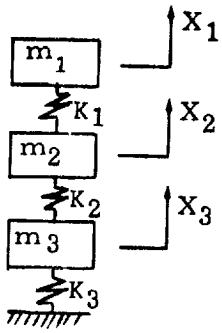

Figure 16. Three Degree of Freedom Spring Mass System

The close coupled system is used for simplicity. By removing spring element K_2, the system is divided into two smaller components. It can be shown by elementary dynamic analysis that the dynamic characteristics of the two component parts are:

	Component 1		Component 2
ω^2	0	$\frac{K_1[m_1 + m_2]}{m_1 m_2}$	$\frac{K_3}{m_3}$
m	$m_1 + m_2$	$\frac{m_1}{m_2}[m_1 + m_2]$	m_3
$\omega^2 m$	0	$K_1\left[\frac{m_1 + m_2}{m_2}\right]^2$	K_3
ψ	1	1	1
	1	$-\frac{m_1}{m_2}$	

The displacements are expressed in terms of the component modes as:

$$X_1 = X_1 + \psi_{11}\,\eta_1$$

$$X_2 = X_1 + \psi_{21}\,\eta_1$$

$$X_3 = \psi_{12}\,\eta_2$$

or

$$\begin{Bmatrix} X_1 \\ X_2 \\ X_3 \end{Bmatrix} = \begin{bmatrix} 1 & \psi_{11} & 0 \\ 1 & \psi_{21} & 0 \\ 0 & 0 & \psi_{12} \end{bmatrix} \begin{Bmatrix} X_1 \\ \eta_1 \\ \eta_2 \end{Bmatrix} = \begin{bmatrix} 1 & 1 & 0 \\ 1 & -\frac{m_1}{m_2} & 0 \\ 0 & 0 & 1 \end{bmatrix} \begin{Bmatrix} X_1 \\ \eta_1 \\ \eta_2 \end{Bmatrix} .$$

The deformation of the connecting element is given by

$$\Delta = X_2 - X_3 = X_1 + \psi_{21}\,\eta_1 - \psi_{12}\,\eta_2$$

or

$$\Delta = \begin{bmatrix} 0 & 1 & -1 \end{bmatrix} \begin{bmatrix} 1 & 1 & 0 \\ 1 & -\frac{m_1}{m_2} & 0 \\ 0 & 0 & 1 \end{bmatrix} \begin{Bmatrix} X \\ \eta_1 \\ \eta_2 \end{Bmatrix}$$

which can be simplified to

$$\Delta = \begin{bmatrix} 1 & -\frac{m_1}{m_2} & -1 \end{bmatrix} \begin{Bmatrix} X_1 \\ \eta_1 \\ \eta_2 \end{Bmatrix} .$$

The contribution of the connecting element to the stiffness matrix is

$$\begin{Bmatrix} 1 \\ -\frac{m_1}{m_2} \\ -1 \end{Bmatrix} [K_2] \begin{bmatrix} 1 & -\frac{m_1}{m_2} & -1 \end{bmatrix}$$

or

$$\begin{bmatrix} K_2 & -\frac{m_1}{m_2} K_2 & -K_2 \\ -\frac{m_1}{m_2} K_2 & \left(\frac{m_1}{m_2}\right)^2 K_2 & \frac{m_1}{m_2} K_2 \\ -K_2 & \frac{m_1}{m_2} K_2 & K_2 \end{bmatrix}$$

The contribution of the component is the diagonal matrix

$$\begin{bmatrix} 0 & & \\ & K_1\left[\frac{m_1 + m_2}{m_2}\right]^2 & \\ & & K_3 \end{bmatrix}.$$

These two are added to form the final stiffness matrix.

The mass matrix is formed directly from the component mode generalized masses,

$$\begin{bmatrix} m_1 + m_2 & & \\ & \frac{m_1}{m_2}\left(m_1 + m_2\right) & \\ & & m_3 \end{bmatrix}$$

The governing equation is thus:

$$\begin{bmatrix} m_1 + m_2 & & \\ & \frac{m_1}{m_2}(m_1 + m_2) & \\ & & m_3 \end{bmatrix} \begin{Bmatrix} \ddot{X} \\ \ddot{\eta}_1 \\ \ddot{\eta}_2 \end{Bmatrix} + \begin{bmatrix} K_2 & -\frac{m_1}{m_2}K_2 & -K_2 \\ -\frac{m_1}{m_2}K_2 & \left(\frac{m_1}{m_2}\right)^2 K_2 + K_1 \left(\frac{m_1 + m_2}{m_2}\right)^2 & \frac{m_1}{m_2}K_3 \\ -K_2 & \frac{m_1}{m_2}K_2 & K_2 + K_3 \end{bmatrix} \begin{Bmatrix} X \\ \eta_1 \\ \eta_2 \end{Bmatrix} = 0$$

To examine the accuracy of this technique applied to this particular model, numerical values may be applied to the system parameters and solutions obtained from the above equations and also from equations derived in the classical manner.

Let M_1 = 10 slugs (143 x 10^6 dynes), M_2 = 20 slugs (286 x 10^6 dynes) M_3 = 30 slugs (429 x 10^6 dynes), K_1 = 15000 lb/ft (224.8 kg/cm), K_2 = 12000 lb/ft (179 kg/cm), K_3 = 10000 lb/ft (149 kg/cm). The eigenvalues and eigenvectors resultant from the two sets of equations are as follows:

	Classical Equation	Mode Synthesis Equa.
Eigenvalue 1	7.6651127×10^{-3}	7.6651123×10^{-3}
Eigenvector 1	$\begin{Bmatrix} 1.00000 \\ 0.91303 \\ 0.60578 \end{Bmatrix}$	$\begin{Bmatrix} 1.00000 \\ 0.91303 \\ 0.60578 \end{Bmatrix}$
Eigenvalue 2	1.1096561×10^{-3}	1.1096558×10^{-3}
Eigenvector 1	$\begin{Bmatrix} 1.00000 \\ 0.39921 \\ -0.95138 \end{Bmatrix}$	$\begin{Bmatrix} 1.00000 \\ 0.39921 \\ -0.95138 \end{Bmatrix}$
Eigenvalue 3	3.9189681×10^{-4}	3.9189677×10^{-4}
Eigenvector 3	$\begin{Bmatrix} 1.00000 \\ -0.70113 \\ 0.15423 \end{Bmatrix}$	$\begin{Bmatrix} 1.00000 \\ -0.70113 \\ 0.15423 \end{Bmatrix}$

5/REFERENCES

1. Bisplinghoff, R.A., H. Ashley and R. L. Halfman, "Aeroelasticity", Addison-Wesley Publishing Company, Reading, Mass., 1955

2. Lukens, D. R., A. F. Schmitt, and G. T. Broucek, "Approximate Transfer Functions for Flexible-Booster-and-Autopilot Analysis, WADD-TR-61-93, April 1961

3. Mills, W. R., "Structural Dynamic Characteristics - WA-133A", Boeing Co. Report DZ-4144, 25 August 1961

4. Turney, R. L. and T. Reed, "Final Report Atlas-Agena-OAO Free-Free Vibration Test at Point Loma Test Site", GD/A Report GD/A-DDE64-032, July 1964

5. Beasley, Donald S., "Vibration Analysis of Saturn C-1 (Version C) (U) NASA Report DA-TN-3-60, 5 Feb. 1960 (Confidential)

6. Kiefling, Larry, "Multiple Beam Vibration Analysis of Saturn I and IB Vehicles", NASA TM X-53072, June 1964

7. Lindberg, James P., "Flight Test Comparison of SA-6 Vehicle Bending and Torsional Dynamics with Dynamic Tests" NASA Memorandum R-AERO-FF-65-4 Jan. 7, 1965

8. Scanlan, Robert H., and Robert Rosenbaum, "Introduction to the Study of Aircraft Vibration and Flutter", The Macmillian Company, New York, N.Y., 1951

9. Myklestad, N.O., "Fundamentals of Vibration Analysis", McGraw-Hill Book Company, New York, N. Y., 1956

10. Thomson, W. T., "Mechanical Vibrations", Prentice-Hall, Inc., Englewood Cliffs, N. J., 1953

11. Rogers, Grover L., "An Introduction to the Dynamics of Framed Structures", John Wiley & Sons, New York, 1959

12. Backus, F. I., "SLV-3 Bending Stability Analysis of the Atlas/Agena Spring Band Separation Joint", GD/A Report GD/A-DDE 64-054, 17 August 1964

13. Silverburg, Samuel, "The Effect of Longitudinal Acceleration Upon the Natural Modes of Vibration of a Beam", STL Report TR-59-0000-00791, August 1959

14. Gravitz, Stanley I., "An Analytical Procedure for Orthogonalization of Experimentally Measured Modes", Journal of the Aerospace Sciences, November 1958

15. Bergen, J. T., "Visco-Elasticity Phenomenological Aspects", Academic Press, 1960

16. Bland, D. R., "Theory of Linear Viscoelasticity", Pergamon Press, 1960

17. Storey, Richard E., "Dynamic Analysis of Clustered Boosters with Application to Titan III" AIAA 1963 Summer Meeting, Paper No. 63-208, June 1963

18. Bodley, Ikard, and Schultz, "Vibration Analysis Report, Program 624A, Configuration C, Flight Plan VIII", Air Force Report No. SSD-CR-65-1, January 1965

19. Milner, James L., "Three Dimensional Multiple Beam Analysis of a Saturn I Vehicle", NASA TM X-53098, July 1964

20. O'Rourke, J. D., and C. Rydz, "Research and Investigative Analysis Using Kron's Method of Analyzing Redundant Structures", Chrysler Corp., Report ADB-TN-29-62, 1 November 1962

21. Bost, R. B., "Saturn Vibration Analysis", Temco Aircraft Corp., Report No. 00304, 22 September 1961

22. Lanczos,C., "An Iterative Method for the Solution of the Eigenvalue of Linear Differential and Integral Operations", Journal of Research of the National Bureau of Standards, Vol. 45, No. 4, October 1950

23. Meissner, C. J.,and R. S. Levy, "Flexibility Method of Coupling Redundant Complex Structures", Journal of the Structural Division, Proceedings of the American Society of Civil Engineers, V89, No. ST6, December 1963

24. Berman, J. H. and J. Sklerov, "Calculation of Natural Modes of Vibration for Free-Free Structures in Three Dimensional Space", AIAA Journal Vol. 3, No. 1, January 1963

25. Meissner, C. J., et al, "The Determination of the Natural Modes of Vibration for Large Systems", Republic Aviation Report No. RAC-406-4, 8 March 1963

26. Glaser, Rudolf F. - NASA Report to be published

27. Lowey, Robert - NASA Report to be published

28. Lianis, George, "Matrix Analysis of Vibrations of Clustered Boosters", GD/A Report AE61-0858, September 1961

29. Gieseke, R. K., B. Appleby and W. Tonelli, "General Missile Vibration Program", GD/A Report GD/A-DDE64-050, 20 August 1964

30. Timoshenko, S. and G. L. MacCullough, "Elements of Strength of Materials", D. Van Nostrand Company, Inc., Princeton, N. J., 1949

31. Bodewig, E., "Matrix Calculus", North Holland Publishing Co., Amsterdam, 1959

32. Faddeeva, V.N., "Computational Methods of Linear Algebra", Dover Publications, N.Y., 1959

NASA-Langley, 1967 —— 32 CR-935